

INVITED REVIEW

Basaltic explosive volcanism: Constraints from deposits and models

B.F. Houghton*, H.M. Gonnermann

Department of Geology and Geophysics, University of Hawai'i at Manoa, Honolulu, HI 96822, USA

Received 13 March 2008; accepted 10 April 2008

Abstract

Basaltic pyroclastic volcanism takes place over a range of scales and styles, from weak discrete Strombolian explosions ($\sim 10^2\text{--}10^3\text{ kg s}^{-1}$) to Plinian eruptions of moderate intensity ($10^7\text{--}10^8\text{ kg s}^{-1}$). Recent well-documented historical eruptions from Etna, Kīlauea and Stromboli typify this diversity. Etna is Europe's largest and most voluminously productive volcano with an extraordinary level and diversity of Strombolian to subplinian activity since 1990. Kīlauea, the reference volcano for Hawaiian fountaining, has four recent eruptions with high fountaining (>400 m) activity in 1959, 1960, 1969 (–1974) and 1983–1986 (–2008); other summit (1971, 1974, 1982) and flank eruptions have been characterized by low fountaining activity. Stromboli is the type location for mildly explosive Strombolian eruptions, and from 1999 to 2008 these persisted at a rate of ca. 9 per hour, briefly interrupted in 2003 and 2007 by vigorous paroxysmal eruptions. Several properties of basaltic pyroclastic deposits described here, such as bed geometry, grain size, clast morphology and vesicularity, and crystal content are keys to understand the dynamics of the parent eruptions.

The lack of clear correlations between eruption rate and style, as well as observed rapid fluctuations in eruptive behavior, point to the likelihood of eruption style being moderated by differences in the fluid dynamics of magma and gas ascent and the mechanism by which the erupting magma fragments. In all cases, the erupting magma consists of a mixture of melt and gaseous bubbles. The depth and rate of degassing, melt rheology, bubble rise and coalescence rates, and extent of syn-eruptive microlite growth define complex feedbacks that permit reversible shifts between fragmentation mechanisms and in eruption style and intensity. However, many basaltic explosive eruptions end after an irreversible shift to open-system outgassing and microlite crystallization in melt within the conduit.

Clearer understanding of the factors promoting this diversity of basaltic pyroclastic eruptions is of fundamental importance in order to improve understanding of the range of behaviors of these volcanoes and assess hazards of future explosive events at basaltic volcanoes. The three volcanoes used for this review are the sites of large and growing volcano-tourism operations and there is a public need both for better knowledge of the volcanoes' behavior and improved forecasting of the likely course of future eruptions.

© 2008 Elsevier GmbH. All rights reserved.

Keywords: Explosive volcanism; Basaltic eruptions; Strombolian; Hawaiian; Subplinian; Plinian

1. Introduction

This review examines “dry” explosive eruptions at basaltic volcanoes, linked to degassing and outgassing of magmatic volatiles; phreatomagmatic explosions

*Corresponding author. Tel.: +1 808 956 2561;
fax: +1 808 956 5512.

E-mail address: bhought@soest.hawaii.edu (B.F. Houghton).

involving an external source of water are not considered here. The review is largely constructed around recent historical activity at Etna, Kīlauea and Stromboli. The last two decades have seen intense pyroclastic activity at these “popular” basaltic volcanoes (Fig. 1) of Kīlauea, with the ongoing Pu‘u ‘O‘o eruption since 1983 (Heliker et al., 2003), Etna with 150 fire fountain episodes since 1990 (Branca and del Carlo, 2005) and major flank eruptions in 2001 and 2002–2003 (Andronico et al., 2005), and Stromboli, with paroxysms in 2003 and 2007 (Calvari et al., 2005; Ripepe et al., 2005; Rosi et al., 2006; Andronico et al., 2007). These volcanoes are the type localities for Strombolian, Hawaiian and basaltic subplinian eruption styles, respectively, but each has a rich diversity of explosive styles, with overlapping ranges of mass discharge rates, which demonstrates the difficulty of applying pigeon hole classifications to the spectrum of basaltic explosive processes in nature.

These eruptions are exceptionally well constrained by direct observations (e.g., Richter et al., 1970; Swanson et al., 1979; Heliker et al., 2003; Landi et al., 2004; Taddeucci et al., 2004a; Andronico et al., 2005; Calvari et al., 2005; Behncke et al., 2006; Rosi et al., 2006) and geophysically (Chouet et al., 1999; Bonaccorso, 2006; Harris and Ripepe, 2007) and geochemically (Garcia

et al., 1992; Metrich et al., 2001; Corsaro and Miraglia, 2005; Shamberger and Garcia, 2006).

2. Styles and intensities of basaltic explosive volcanism

2.1. Classifying basaltic explosive eruptions

The most widely cited classifications for explosive eruptions (Walker, 1973; Pyle, 1989) utilize a combination of some proxy for eruption intensity/mass discharge rate and some measure of particle size. Walker (1973) was the first to recognize the value of fall deposit geometry as a proxy for eruption intensity/discharge rate (Fig. 2). He linked deposit geometry (via D , the area over which a deposit thins to 0.01 of its thickness maximum) to mass discharge rate/intensity and inferred that a spectrum of “dry” or “magmatic” pyroclastic deposits from Hawaiian to Strombolian to subplinian to Plinian could be distinguished in terms of a steady increase in D and, thus, mass discharge rate. This classification has been used widely, because it employs simple parameters that can be derived from pyroclastic



Fig. 1. Images illustrating the diversity of basaltic explosive volcanism. (a) Kīlauea Iki 1959, Episode 3. High fountaining eruption on 29 November 1959. Photograph Jerry Eaton. (b) Etna 20 July 2001 showing three contrasting styles of eruption from vents on the 2001 eruption fissure. In the foreground weak Strombolian explosions from the principal vent at 2100m elevation. Weak phreatomagmatic activity occurs from an adjacent vent to the left (west). In the background the initiation of a more powerful phreatomagmatic explosion with subplinian dispersal at the 2500m vent. Photograph Bruce Houghton. (c) Typical moderate intensity explosion of Stromboli, 23 July 2007. Photograph Tom Pfeiffer.

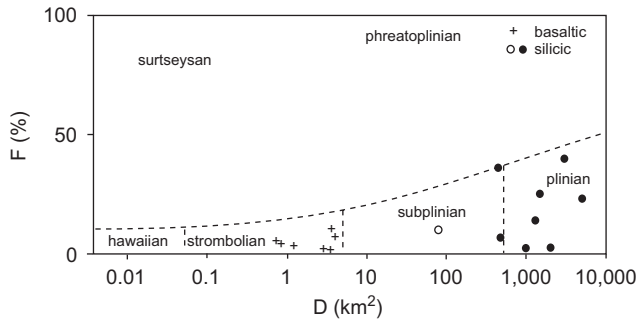


Fig. 2. Classification of explosive eruptions after the benchmark Walker (1973) paper. D is a measure of thinning rate (see text). F is a measure of the grain size of the deposit – the percentage of material finer than 1 mm at the point where the $0.1T_{\max}$ isopach crosses the dispersal axis (where T_{\max} is the maximum thickness of the deposit). Note that no Hawaiian data are presented. Fields for Strombolian, subplinian and Plinian eruptions are defined on quantitative data, but the Hawaiian field reflects qualitative field observations, and would exclude all powerful historical Hawaiian eruptions.

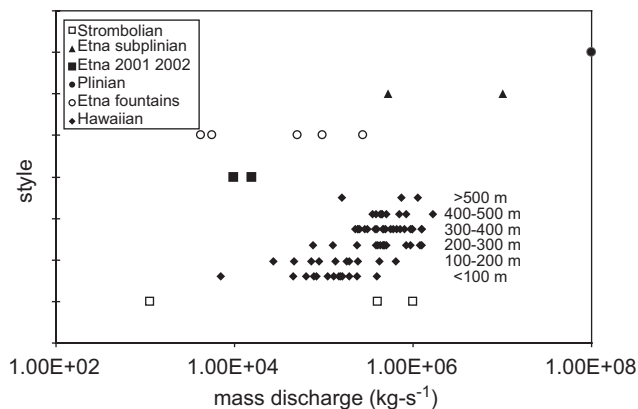


Fig. 3. Plot of mass discharge rate for eruptions of different style at Stromboli, Kīlauea and Etna. For Hawaiian eruptions only eruptions or episodes from single point-source vents are included. Hawaiian data are organized into subsets by maximum recorded fountain height (0–100, 100–200 m, etc.). There were insufficient data points to do this for the other eruptive styles. At Etna we have subdivided subplinian events (after Branca and del Carlo, 2005) from events characterized by fountaining that was more similar to the Hawaiian eruptions at Kīlauea.

deposits irrespective of whether eye-witness accounts exist for the eruptions.

Unfortunately, mass discharge rates for well-documented examples of the classical eruption styles described above have wide and overlapping ranges of values (Fig. 3). This was not apparent because the Walker (1973) and other existing classifications lack data for Hawaiian eruptions. Walker (1973) chose to represent Hawaiian eruptions as weaker than Strombolian events (Fig. 2). However, his plot shows clearly that

his data did not include any Hawaiian eruptions nor did he include any eruptions of Stromboli itself. Data now available (Fig. 3) suggest that there is a total overlap in time-averaged discharge rates between Strombolian and Hawaiian eruptions, and that some other criteria are needed to distinguish them and their products. For example, our analysis of 99 eruptions or eruption episodes at Kīlauea since 1955 shows a range of time-averaged discharge rates between 4×10^2 and 10^6 kg s^{-1} . Fewer data are available from Strombolian explosions, but discharge rates as low as $10\text{--}500 \text{ kg s}^{-1}$ are typical for “normal” explosions at Stromboli (Chouet et al., 1973; Ripepe et al., 1993; Allard et al., 1994) and as high as $10^5\text{--}10^6 \text{ kg s}^{-1}$ for paroxysms (Rosi et al., 2006). Available data suggest that Strombolian explosions at other volcanoes occupy the middle ground between typical and paroxysmal eruptions at Stromboli. For example, explosions at Arenal between 1987 and 2001 (Cole et al., 2005) had average discharges of approximately $10\text{--}50 \text{ m}^3$ per explosion, roughly equivalent to $10^3\text{--}10^4 \text{ kg s}^{-1}$.

Observers have recognized that the fundamental distinction between Strombolian and Hawaiian eruptions is not dispersal rate but steadiness of discharge rate, with the former being impulsive short-lived discrete events (Chouet et al., 1973; Blackburn et al., 1976; Patrick et al., 2007) and the latter expressed as sustained fountaining events where discharge rates are maintained for hours to days (Richter et al., 1970; Swanson et al., 1979; Heliker et al., 2003). This distinction between these styles is commonly not possible by use of parameters like D which reflect intensities averaged over entire eruptions or eruption episodes.

2.2. Case studies

Kīlauea’s most recent pyroclastic history includes three eruptions with high fountaining (>400 m) activity in 1959, 1969–1974 and 1983–2007 (Richter et al., 1970; Swanson et al., 1979; Heliker et al., 2003). These eruptions have also included intervals of weaker fountaining, building highly localized spatter ramparts, and periods of gas pistoning and persistent passive degassing. Other eruptions (Duffield et al., 1982; Macdonald et al., 1984) have been characterized by only low fountaining activity (e.g., 1971, 1974, 1982).

Stromboli is the type location for mildly explosive Strombolian eruptions (Barberi et al., 1993). Explosive events have persisted at least since 600 AD (Rosi et al., 2000), and from 1999 to 2003 persisted at a rate of ca. 9 per hour (Harris and Ripepe, 2007). This pattern of activity, with alternating ash-rich and scoria-rich explosions, was briefly interrupted in 2002–2003 and 2007 by episodes of both lava effusion and vigorous paroxysmal Strombolian eruptions.

Etna has shown an extraordinary level of explosive activity in the last 2 decades (Coltelli et al., 2000). The duration of eruptions has lasted between days and weeks, with time-averaged discharge rates between 10^3 and 10^6 kg s^{-1} (Andronico et al., 2007; Alparone et al., 2007). More than 150 fountaining episodes have occurred since 1990, the strongest of which formed plumes 2–13 km high, had ejecta volumes of 10^4 – 10^7 m^3 , and discharge rates that equate to intense Strombolian to subplinian in intensity (sensu Walker, 1973; Pyle, 1989). Other sustained but generally lower fountains have alternated with periods of rapid discrete explosions described by observers as Strombolian in character. Etna's explosivity thus spans a middle ground, overlapping with end-member styles of subplinian, Hawaiian and Strombolian volcanism. Single eruptions such as those in 2001 and 2002–2003 have displayed this full range of explosivity, with contrasting eruption styles at adjacent vents (Fig. 1), or at a single vent on time scales of days. In addition, a number of ash-producing events (Taddeucci et al., 2004a, b) in 2001 and 2002 do not fit well with the existing end-member names. A key question is to what extent the discrete, impulsive explosions at Etna can be equated to Strombolian explosions (as typified by Stromboli) and to what extent the less powerful sustained fountains are similar to Kīlauea's fountaining behavior.

2.3. Typical Strombolian eruptions

The activity considered typical of Stromboli represents the mild end-member of Strombolian explosions as

defined by Walker (1973). It consists of prolonged sequences of impulsive short-lived explosions (Figs. 4a and b), lasting a few seconds to tens of seconds and ejecting ash to bombs to heights of typically less than 200 m (Barberi et al., 1993). Individual explosions eject typically between 0.01 and 10 m^3 of pyroclasts, equivalent to average discharge rates of 1 – 10^4 kg s^{-1} (Chouet et al., 1973; Ripepe et al., 1993). At Stromboli and other volcanoes activity is often distributed over several adjacent vents (Cole et al., 2005) that may erupt with contrasting styles and intensities. The most detailed study of an extended period of explosions is that by Patrick et al. (2007) of 135 explosions at Stromboli in June–July 2004. Eruption durations ranged from 6 to 41 s (mean $15 \pm 6 \text{ s}$), jet heights were up to 180 m, and exit velocities were between 3 and 100 m s^{-1} (mean $24 \pm 19 \text{ m s}^{-1}$). During this period, explosions were observed from vents in each of the three summit craters; Fig. 5 summarizes data for only explosions from the NE crater for short periods of observations on each of 2 days.

Strombolian explosion frequency at other volcanoes can be both significantly greater and more irregular – for example up to 93 explosions per day at Arenal in the last 20 years with volumes of ~ 10 – 50 m^3 and with gaps of up to 3 weeks without explosions (Cole et al., 2005) and with greater average intensities and dispersals (Fig. 6) only achieved at Stromboli during paroxysms.

In Strombolian eruptions, it is thought that at low magma ascent rates, relative to bubble rise velocities and significant dynamical interaction between bubbles results in bubble coalescence to form gas slugs. In two

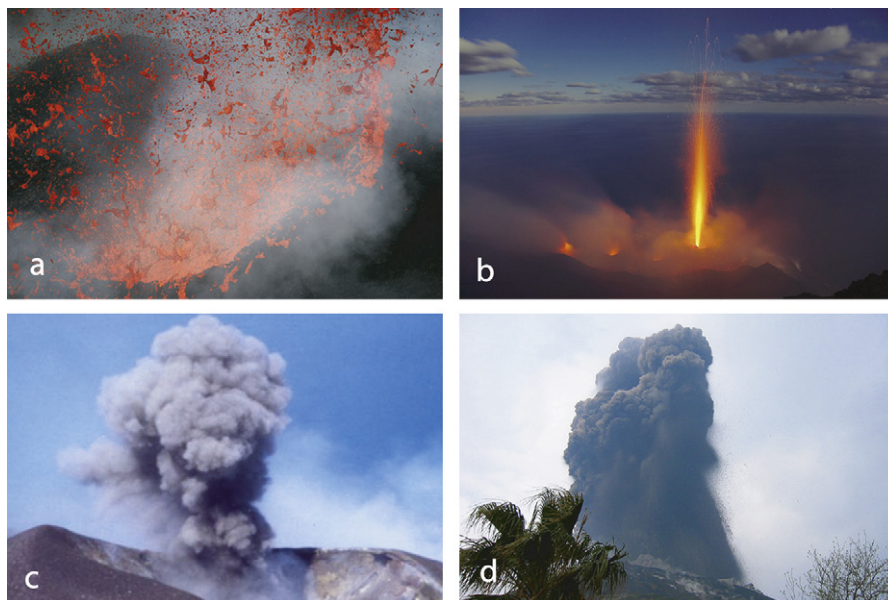


Fig. 4. Examples of typical and atypical explosions at Stromboli. (a) Weak, type 1 explosion, 1 January 2006. Photograph Tom Pfeiffer. (b) Powerful, collimated type 1 explosion with +300 m jet, 5 November 2006. Photograph Marco Fulle. (c) Ash-rich, type 2 explosion. Photograph Mathew Patrick. (d) Strombolian paroxysm on 5 April 2003 at 7:13 a.m. GMT. Photograph Andreas Franssen.

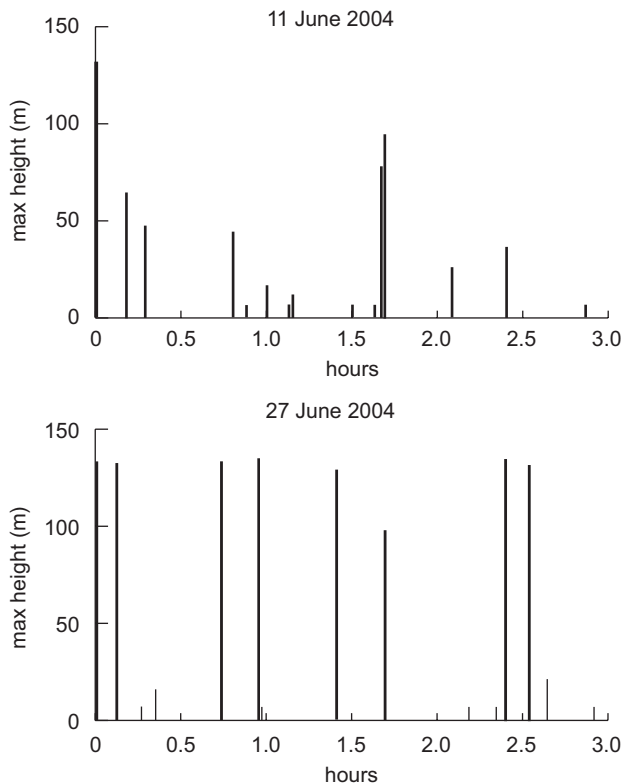


Fig. 5. Heights and timings of recorded explosions at Stromboli NE crater on 11 and 27 July 2004, after Patrick (1996). Note no attempt is made to depict the duration of explosions which ranged between 6 and 41 s.

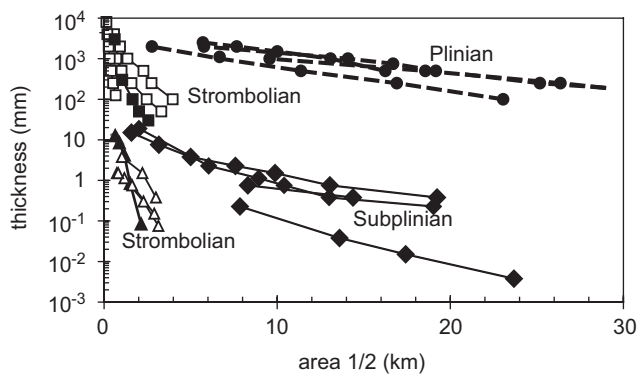


Fig. 6. Plot of tephra thickness versus $\text{area}^{1/2}$ for selected basaltic pyroclastic deposits. Strombolian deposits have open symbols (squares from Walker (1973); triangles recent Arenal Strombolian fall deposits from Cole et al. (2005)); the closed symbols and bold line is the Etna 2003 paroxysm). 1959 Kilauea Iki eruption closed squares. Recent subplinian deposits of Etna are diamonds. Basaltic Plinian eruptions solid circles. Where only isomass data were available, they were converted into thickness equivalents using field measurements of bulk density for the deposits.

contrasting models (Fig. 7), slugs either form dynamically during rise through the conduit (e.g., Wilson and Head, 1981; Parfitt, 2004; Parfitt and Wilson, 1995;

Parfitt et al., 1995) or by foam collapse at the shoulder connecting conduit and magma chamber (e.g., Vergnolle and Jaupart, 1986, 1990; Jaupart and Vergnolle, 1988, 1989). In both cases, slug formation can be enhanced or facilitated at geometric asperities within the magmatic plumbing system (James et al., 2004). Large gas slugs rise to the surface at much faster rates than the melt, resulting in a relatively volatile-depleted magma in the shallow conduit (Lautze and Houghton, 2005, 2006) and Strombolian style eruptions when the bubbles burst at the surface (e.g., Blackburn et al., 1976; Wilson, 1980; Vergnolle and Brandeis, 1994; Vergnolle et al., 1996; Chouet et al., 2003; Harris and Ripepe, 2007; Patrick et al., 2007). In Strombolian eruptions, the explosion is simply the consequence of rupture of the over-pressured large gas slug at the magma surface, mechanically distinct from the inertial mechanisms by which magma may fragment during Hawaiian eruptions (e.g., Namiki and Manga, 2008).

Therefore, the key to the dynamics and occurrence of the Strombolian style of behavior appears to be degassing, the segregation and mechanical decoupling of the exsolved gas phase, and subsequently the dynamics of ascent of the gas as discrete, large slugs (e.g., Wilson and Head, 1981; Parfitt, 2004; Parfitt and Wilson, 1995). From a fluid-dynamical point of view, it is known that small perturbations in gas–liquid flow systems can lead to significant oscillations in flow rates and flow regimes (e.g., Baker, 1954; Taitel et al., 1980; Tutu, 1982, 1984; Furukawa and Fukano, 2001; Cheng et al., 2002; Hibiki and Ishii, 2003a, b; McNeil and Stuart, 2003, 2004; Hu and Golan, 2004; Guet and Ooms, 2006; Guet et al., 2006; Ornebere-Iyari et al., 2007), with strong dependencies on rheology and relative proportions of gas to liquid phase, which may arise as a consequence of volatile solubility, bubble coalescence and magma–dynamic feedbacks throughout the conduit. Such intrinsic dynamical effects that may give rise to the previously discussed observations of intermittent behavior, but have not been fully explored to date.

2.4. Variations on the Strombolian theme

2.4.1. Major variations in style

At Stromboli explosions are frequently either lapilli-rich or ash-rich, referred to as type 1 and type 2, respectively (Chouet et al., 1999; Ripepe and Marchetti, 2002; Marchetti and Ripepe, 2005). The former are the classical form of explosion considered typical of Strombolian eruptions, whereas the latter, while common at Stromboli, are too rich in ash to meet the Strombolian criteria of Walker (1973) and Pyle (1989). Long periods at Stromboli are characterized by a predominance of type 1 explosions from one crater,

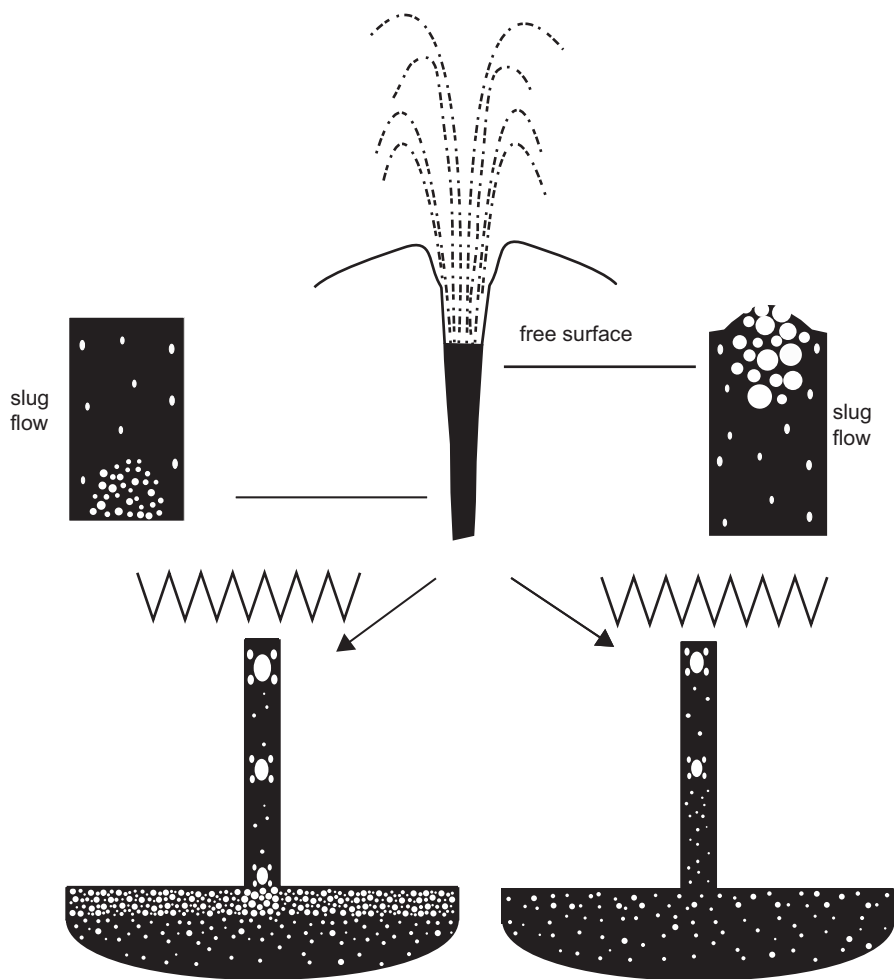


Fig. 7. Cartoon model for Strombolian explosions. Lower diagrams contrast the foam-collapse model of Vergnolle and Jaupart (left) with the rise speed dependent model of Parfitt and Wilson (right).

and type 2 explosions at an adjacent crater (Chouet et al., 1999; Ripepe and Marchetti, 2002; Marchetti and Ripepe, 2005). Both explosion types form an incandescent jet, but type 2 explosions generate both a jet and a weak convective plume typically extending to a few kilometers height (Patrick et al., 2007). There is some controversy concerning the origin of the type 2 explosions, as to whether the pyroclasts represent relatively viscous and stagnant melt or whether many are recycled through fallback and/or collapse of the conduit walls.

2.4.2. Major variations in intensity

Every few decades (e.g., 1930, 1950, 2003, 2007) Stromboli experiences a more powerful short-lived explosive eruption termed a paroxysm (Barberi et al., 1993). Weaker paroxysms were recorded in September 1996, August 1998 and August 1999 (Metrich et al., 2005). Mass discharge rates are typically two or three orders of magnitude higher than the “typical” Strombolian behavior described above and may reach discharge rates as high as 10^5 – 10^6 kg s^{-1} (Rosi et al., 2006). They tap a deeper, hotter, crystal-poor magma

that largely bypasses the shallow storage region at Stromboli (Metrich et al., 2005) and possibly are driven by episodic open-system outgassing of CO_2 -rich gas from depths of several kilometers (Allard, 2007).

2.5. Typical Hawaiian eruptions

Typical Hawaiian behavior is popularly pictured to be the episodic fountaining events (Richter et al., 1970; Swanson et al., 1979; Heliker et al., 2003) to heights of > 300 m (Fig. 8) like the 1959 Kīlauea Iki, 1969–1974 Mauna Ulu and 1983–present Pu‘u ‘O‘o eruptions (Table 1). Typically any one eruption will have multiple episodes of continuous magma discharge separated by pauses that are typically longer than the duration of the episodes (e.g., Fig. 9). We have compiled data on erupted volume, average mass discharge rate, and duration for 79 eruptive episodes in 1959, 1969 and 1983–1986 (Fig. 10). For comparison we also show data from another 20 historical eruptions from Kīlauea. The highest average mass discharge rates are predictably

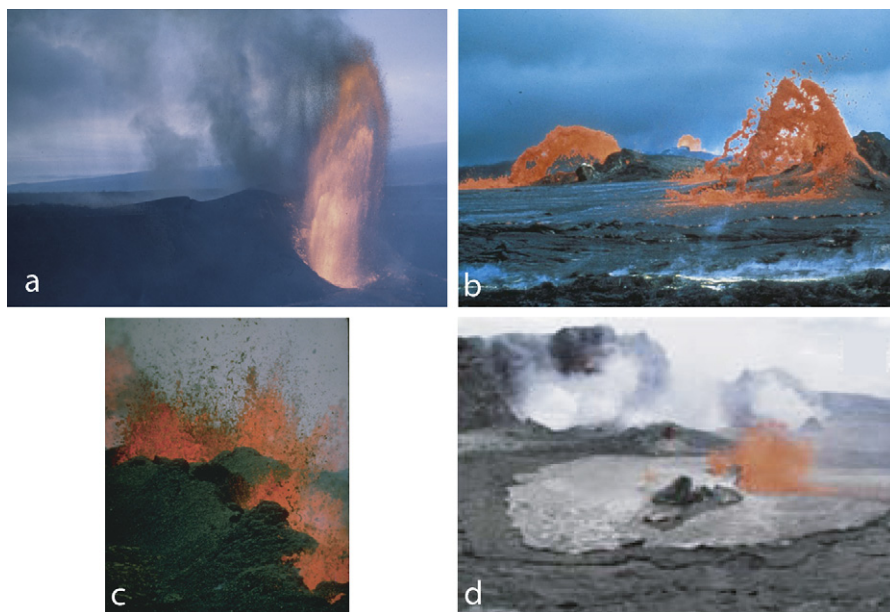


Fig. 8. Images of Hawaiian explosive eruptions. (a) 450 m high fountain at Kīlauea Iki at 7:00 a.m. on 29 November 1959 (Episode 3) with downwind drift of ejecta to the south. Photograph Jerry Eaton. (b) Mauna Ulu ‘dome’ fountain on 29 June 1970. Photograph Don Swanson. (c) Weak spattering activity at Mauna Loa, 6 March 1984. Photograph J.D. Griggs. (d) Gas pistoning eruption at Pu‘u ‘O‘o. Photograph Marie Edmonds.

Table 1. Summary parameters for three high fountaining eruptions of Kīlauea

| | Eruption | | |
|--|-------------------------|--------------------|--------------------|
| | Kīlauea Iki (1983–1986) | Pu‘u ‘O‘o (1959) | Mauna Ulu (1969) |
| Number of high fountaining episodes | 16 | 45 | 12 |
| Average episode duration (h) | 20 ^a | 43 | 18 |
| Maximum episode duration (h) | 167 | 384 | 34 |
| Average of maximum fountain height (m) | 314 | 256 | 229 |
| Maximum fountain height recorded (m) | 579 | 467 | 540 |
| Average discharge rate (kg s ⁻¹) | 7.8×10^5 | 1.5×10^5 | 4.7×10^6 |
| Highest average discharge rate (kg s ⁻¹) | 1.7×10^6 | 9.7×10^5 | 1.2×10^6 |
| Duration of high fountaining phase (d) | 36 | 1271 | 221 |
| Time in high fountaining eruption (d) | 13 | 47 | 10 |
| Total duration of eruption (d) | 36 | 9114+ | 874 |
| Volume for high fountaining episodes (m ³) | 1.50×10^8 | 5.00×10^8 | 6.50×10^7 |
| Total volume (m ³) | 1.50×10^8 | 1.20×10^9 | 1.85×10^8 |

^aFor Kīlauea Iki episode 1 is atypically long; the average minus episode 1 is 10 h. “Duration of high fountaining phase” is the total elapsed time since the onset of the eruption, i.e., it includes the pauses between episodes. “Time in high-fountaining eruption” is the aggregate time spent in high eruption across all episodes. Data from Richter et al. (1970), Swanson et al. (1979) and Heliker et al. (2003).

associated with these three high fountaining events (Fig. 3), but similar values are associated with some fountaining eruptions from extended fissure sources which rarely exceeded heights of 100–200 m.

There is similarity but also significant diversity amongst these three high fountaining eruptions. The Kīlauea Iki eruption was very short-lived and characterized only by intense high fountaining; in the other two eruptions, early high fountaining was followed by longer phases of low fountaining and/or lava effusion.

Maximum fountain heights and, more significantly, average fountain heights and erupted volumes, were similar for the high fountaining phases of the three eruptions. The high fountaining portion of each eruption consisted of a number of relatively short eruption episodes separated by significantly longer pauses (e.g., Figs. 9 and 11). In all three eruptions, some of the highest fountaining episodes occurred towards the end of the high fountaining phase. The average durations of episodes were 20, 43 and 18 h and of the pauses 1.5, 18

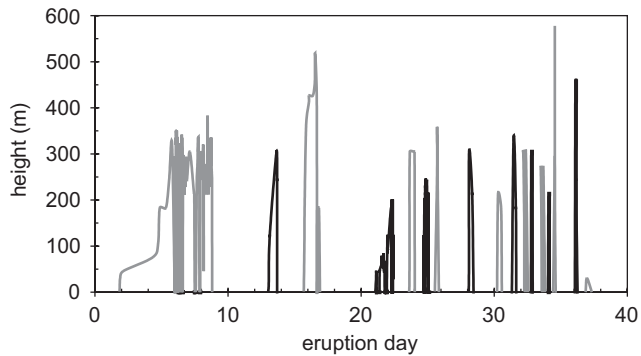


Fig. 9. Plot of fountain height with time for Kīlauea Iki 1959 eruption. Alternate episodes are outlined in gray and black for clarity. Data from Richter et al. (1970) and unpublished Hawai'i Volcanoes National Park records.

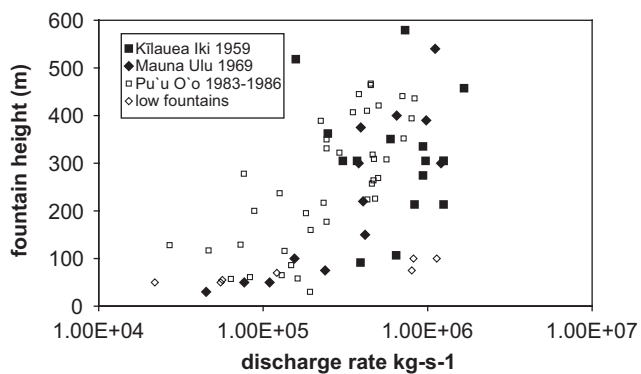


Fig. 10. Plot of maximum fountain height versus average mass discharge rate for high fountaining episodes of the Kīlauea Iki, Mauna Ulu and Pu'u 'O'o eruptions. Also shown for comparison are data for several low fountaining eruptions at Kīlauea (Richter et al., 1970; Duffield et al., 1982; Macdonald et al., 1984; Swanson et al., 1979; Heliker et al., 2003).

and 24 days, respectively, for Kīlauea Iki, Mauna Ulu and Pu'u 'O'o (Richter et al., 1970; Swanson et al., 1979; Heliker et al., 2003). There were considerable fluctuations in fountain height during episodes (e.g., Figs. 9 and 11) that attest to the relative unsteadiness of Hawaiian fountains.

There are two conceptual models for Hawaiian eruptions (Fig. 12). Some workers (e.g., Wilson, 1980; Wilson and Head, 1981; Parfitt, 2004; Parfitt and Wilson, 1995; Parfitt et al., 1995; Slezin, 2003) propose that Hawaiian eruptions are characterized by the presence of bubbles whose buoyant rise is slow relative to the melt phase, that is they are coupled to the melt, resulting in a highly vesicular foam that is disrupted when bubble overpressure exceeds the tensile strength of the intervening melt films. A second school suggests that foam collects and collapses at the contact between the conduit and magma storage zone resulting in annular two-phase flow of gas and melt up the conduit

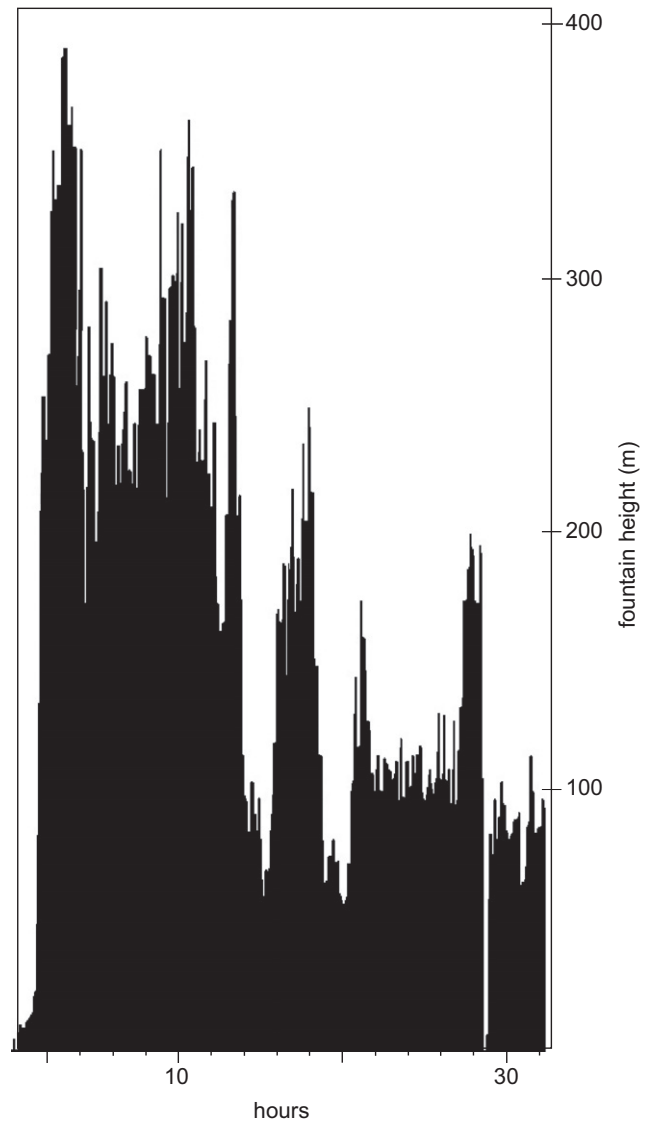


Fig. 11. Fountain height with time for Pu'u 'O'o episode 16, data from Wolfe et al. (1987). After a relatively sharp onset fountain height decays exponentially with time over approximately 30 h, but with substantial fluctuations on a time scale of minutes.

(Vergnolle and Jaupart, 1986, 1990; Jaupart and Vergnolle, 1988, 1989; Vergnolle and Mangan, 2000).

2.6. Variations on the Hawaiian theme

A number of historical eruptions of Kīlauea have lacked high fountaining phases and have been characterized by fountaining to heights often less than 100 m and often from fissure sources (Duffield et al., 1982; Macdonald et al., 1984), building spatter ramparts and feeding lava flows (e.g., 1971, 1974, 1982). Total mass discharge rates from some of these eruptions rival those of the high fountaining eruptions because of the extended length of the fissure source, e.g., the 14 August

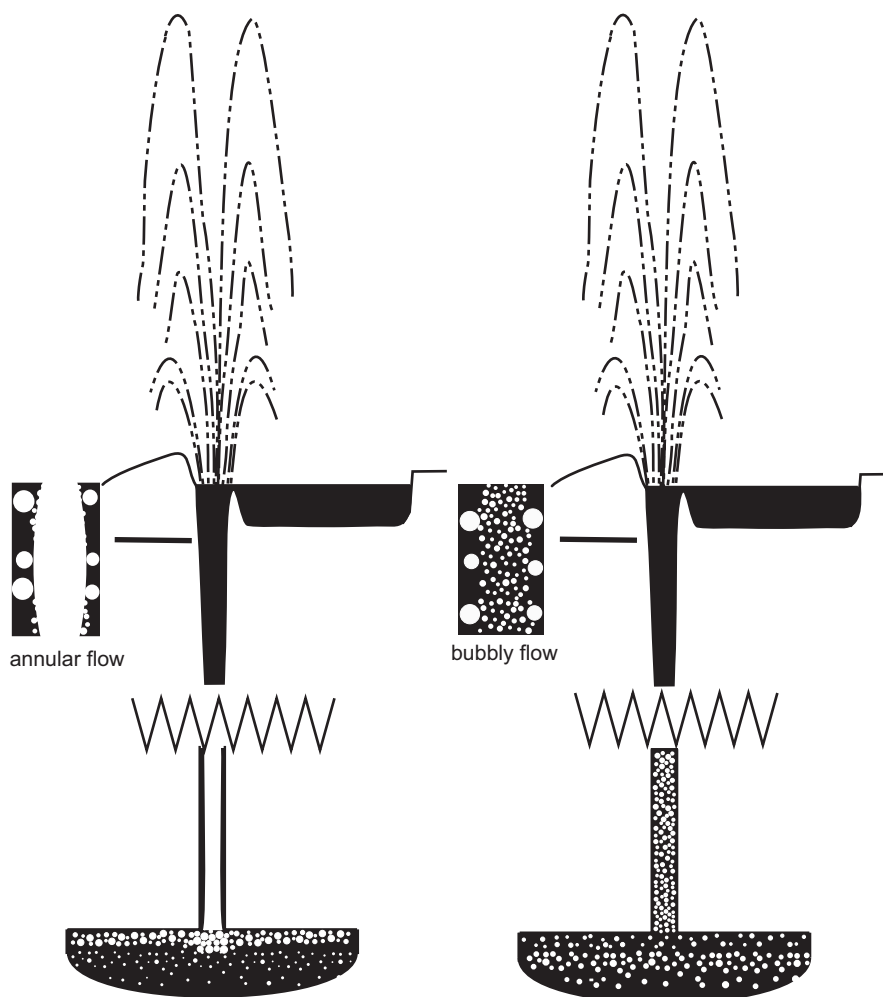


Fig. 12. Cartoon of Hawaiian fountaining. Left the collapsing foam model of Verniolle and Jaupart leading to annular flow. Right the rise speed dependent model of Parfitt and Wilson producing bubble flow.

1971 summit eruption had a mass discharge rate of $8 \times 10^5 \text{ kg s}^{-1}$ (Duffield et al., 1982), but only achieved fountain heights of 20–75 m. Activity is often much less sustained during periods of such low discharge than for the high fountaining eruptions (e.g., 1959, 1969 and 1983–1986). At these times, weak fountaining alternates with discontinuous spattering, and discrete gas pistoning events (and intervals of persistent continuous degassing) (Swanson et al., 1979; Goldstein and Chouet, 1994). Discontinuous spattering events are impulsive transient events ejecting small volumes of coarse ejecta and gas to heights of a few meters or tens of meters (Edmonds and Gerlach, 2007). They are identical to the weakest form of Strombolian explosions as described from Stromboli (Harris and Ripepe, 2007), and Villaricca (Gurioli et al., in press). During gas pistoning, a standing column of lava rises slowly to fill the vent and discharge before draining back rapidly, accompanied by spattering and gas discharge. Edmonds and Gerlach (2007) attribute these contrasting behaviors to contrasting styles of gas-slug formation in the conduit, with gas pistoning

associated with deeper segregation of CO_2 -rich slugs, and spattering explosions with shallow escape of over-pressured water-rich bubbles.

2.7. Subplinian and Plinian basaltic eruptions

Etna is unique amongst active basaltic volcanoes in its frequency of sustained subplinian eruptions; nine occurred in the 20th century and seven since 1990 (Branca and del Carlo, 2005). This very recent history includes two forms of activity of subplinian intensity. In the majority of eruptions “dry” subplinian phases from one or more of the summit craters occur in sequences of paroxysmal eruptions, the majority of which do not attain subplinian intensity (e.g., Carveni et al., 1994; La Volpe et al., 1999; Polacci et al., 2006). Each paroxysm begins with a period of Strombolian explosions of increasing intensity culminating in either powerful fountaining or a sustained subplinian plume. Activity then reduces abruptly to discrete Strombolian explosions.

The 2001 and 2002–2003 flank eruptions took different forms in which the phases characterized by sustained, generally ash-rich plumes have generally been considered to be phreatomagmatic in origin (Taddeucci et al., 2004a,b; Gresta et al., 2004; Andronico et al., 2005; Scollo et al., 2007). In the subplinian eruptions between 1990 and 2000, discharge rates of between 5×10^5 and 10^7 kg s^{-1} were sustained for typical time scales of 0.5–10 h. The subplinian phases typically occur during clusters of fountaining events of lesser intensity, e.g., the eruption of 23 December 1995 over ~ 4.5 h, which produced a jet to 500–600 m feeding a convective plume to 6 km height, was the sixth of ten episodes at Etna's Northeast crater between 9 November 1995 and 25 June 1996 (La Volpe et al., 1999).

Another well-documented basaltic subplinian eruption occurred at Ruapehu volcano on 17 June 1996. Two phases of 3.5 and 2.5 h duration had an averaged mass discharge rate of $5 \times 10^5 \text{ kg s}^{-1}$ and produced a wind-attenuated fall deposit extending at least 300 km to the northeast of the volcano (Bonadonna and Houghton, 2005; Bonadonna et al., 2005).

Plinian eruptions are the rarest and the least well-studied type of basaltic activity, and potentially the most dangerous. Four Plinian eruptions have been characterized in detail: the 122 BC Etna (Coltelli et al., 1998; Houghton et al., 2004; Sable et al., 2006a), the 1886 Tarawera (Walker et al., 1984; Houghton et al., 2004; Sable et al., 2006b, in press; Carey et al., 2007); the ~ 2 ka San Judas (Williams, 1983; Bice, 1985; Perez and Freundt, 2006) and the ~ 60 ka Fontana (Williams, 1983; Bice, 1985; Wehrmann et al., 2006; Costantini et al., in press) eruptions. Inferred plume heights for these eruptions are 20–32 km (Walker et al., 1984; Coltelli et al., 1998; Costantini et al., in press) with volumes of a few km^3 . For Tarawera, the only well-documented eruption, the mean discharge rate was $8.5 \times 10^7 \text{ kg s}^{-1}$ (Walker et al., 1984). Parfitt and Wilson (1999) point out some similarities between Hawaiian and Plinian ascent processes, but Plinian and subplinian eruptions require somewhat unusual conditions to account for the fact that their mass discharge rates are three to five orders of magnitude higher than those of Hawaiian eruptions. Textural observations described in Section 3.4 below favor a hypothesis that abundant microlites significantly increased melt viscosity (Fig. 13), resulting in viscosity-limited bubble growth and the built-up of sufficient gas overpressure for magma fragmentation during ascent-driven decompression (Gonnermann et al., in press).

3. Basaltic pyroclastic deposits

The properties of pyroclastic deposits have been used to classify explosive eruptions in a quantitative fashion. Here we review the most important of those parameters.

3.1. Geometry

Most existing classification schemes use thinning rate with distance from source as a proxy for eruptive intensity, i.e., mass discharge rate. If a deposit exhibits exponential thinning then its dispersal can be characterized by a unique “half-distance” over which the deposit thins to half of its previous thickness. More recent studies showed that many deposits have more complex geometries that are better fitted by several exponential line segments, which Bonadonna et al. (1998) attribute to contrasting settling behaviors for particles of different diameter. New data from recent eruptions (Fig. 6) enable us to evaluate both the relationship between mass discharge rate and deposit geometry and the assumption of exponential thinning. The products of well-documented historical eruptions often contain both cone-building and sheet forming elements over the entire range of mass discharge rates, but the proportion of mass partitioned into the cone varies inversely with eruption intensity – e.g., 94% for the Hawaiian fire fountains of Kīlauea Iki 1959 versus 1% for the 1886 Plinian eruption of Tarawera.

All Strombolian and Hawaiian eruptions are principally cone-forming, as pointed out by Walker (1973). Many such deposits do not follow simple exponential thinning relationships as shown on plots of thickness–area^{1/2} (Fig. 6), where the data are better fitted by power law relationships. This is perhaps predictable as a simple exponential thinning relationship would require, *a priori*, a constant release height of clasts from the jet or fountain, something which is seldom if ever attained in nature in cone-forming eruptions. The effect of superimposing multiple small packages of tephra with different release heights and often different wind conditions and thus following different dispersal patterns is to create a thinning relationship in which more powerful explosions contribute disproportionately to the thickness of the distal deposit.

For the medial to distal products of basaltic Plinian falls (Fig. 6), the Etna 122 BC lapilli fall has a thinning half-distance (b_t) of 2.7 km (Coltelli et al., 1998), Tarawera 1886 has a b_t value of 4.3 km (Sable et al., 2006b) and the Fontana Lapilli has values of 2, 5 and 6 km for unit B, C and D+E+F, respectively (Costantini et al., in press). These values are mostly derived for the medial field as there are few or no distal exposures in every case. There is surprisingly little difference between the subplinian and Plinian deposits described here in this regard.

3.2. Grain size

Physical volcanology utilizes two types of grain size data: individual measurements made on small samples

over limited stratigraphic intervals at single sites, and “whole deposit” data where the grain size of the entire clast population is estimated by assembly of many individual analyses. The former are extremely useful in reconstructing processes of pyroclast transport and sedimentation and fluctuations in mass discharge rate and wind velocity with time. Changes in maximum clast size with distance from vent, particularly cross-wind, are routinely used in estimates of eruption column height and mass flux (e.g., Carey and Sparks, 1986; Wilson and Walker, 1987; Pyle, 1989). Whole deposit grain size data can be used to look at the efficiency and nature of fragmentation (e.g., Parfitt and Wilson, 1999; Bonadonna and Houghton, 2005).

A characteristic of the products of “dry” or “magmatic” explosivity is that individual tephra samples show log-normal unimodal grain-size distribution and are relatively coarse-grained and often better sorted (Fig. 14) with respect to products of those phreatomagmatic explosions, where magma interacts with abundant external water (Surtseyan and phreatoplinian eruptions). Strombolian samples are generally the coarsest with median diameters of typically 16–64 mm whereas Hawaiian samples plot at 2–16 mm (Houghton et al., 2000); both show moderate sorting, i.e., sorting coefficients (σ_ϕ) of less than 2.0. Basaltic Plinian samples have typical median diameters of 4–64 mm and generally moderate sorting ($\sigma_\phi \leq 1.5$) and typically are very uniform with time (Walker et al., 1984; Carey et al., 2007). In comparison the median diameters of “wet” or phreatomagmatic basaltic fall deposits are typically less than 4 mm and σ_ϕ can be as large as 4.0 (Walker and Croasdale, 1972; Houghton et al., 2000).

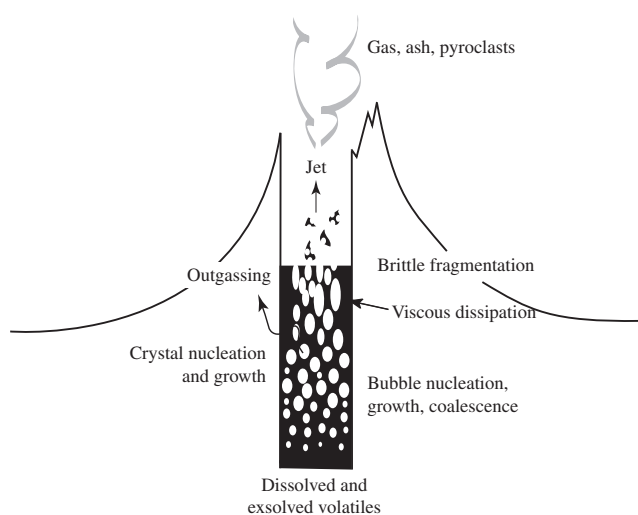


Fig. 13. Cartoon of basaltic Plinian eruption, in which high magma viscosity is achieved as the result of microlite crystallization due to effective undercooling. The high viscosity inhibits bubble rise and promotes brittle fragmentation of the crystal-and-bubble rich magma.

3.3. Juvenile clast morphology

The morphology and shape of juvenile (or magmatic) particles is strongly influenced by melt viscosity and vesicle content at explosive fragmentation (Heiken and Wohletz, 1985; Taddeucci et al., 2004a), but there are few quantitative studies of the shapes of Hawaiian, Strombolian and basaltic Plinian pyroclasts. Across this spectrum of eruption style, there is a progressive decrease in the abundance of aerodynamically shaped fluidal pyroclasts and an increase in the abundance of ragged scoria or pumice (Fig. 15). This reflects the relative viscosity of the erupted magmas, which may be as low as a few hundred Pa s for Hawaiian eruptions, thousands of Pa s for Strombolian eruptions and probably several orders of magnitude higher for basaltic Plinian eruptions (Gonnermann et al., *in press*). The higher vesicle number densities of Plinian clasts (see Section 3.4) also contribute to high degrees of surface roughness.

3.4. Vesicularity and crystallinity

Diverse vesicle and microlite populations in basaltic pyroclasts are sensitive indications of complexity of conduit processes in most basaltic eruptions, implying a delicate balance between mechanical coupling and uncoupling of the gas phase from the rising melt.

There are few quantitative vesicularity data for basaltic pyroclastic deposits except for the pioneering work at Kīlauea (Mangan et al., 1993; Cashman and Mangan, 1994; Mangan and Cashman, 1996) and very recent studies at Stromboli (Lautze and Houghton, 2005, 2006, 2007; Polacci et al., 2008), Etna (Sable et al., 2006a) and Tarawera (Sable et al., *in press*). These data (Fig. 16) show no significant increase in bubble number density with eruption intensity for Hawaiian and Strombolian eruptions with a typical range of number

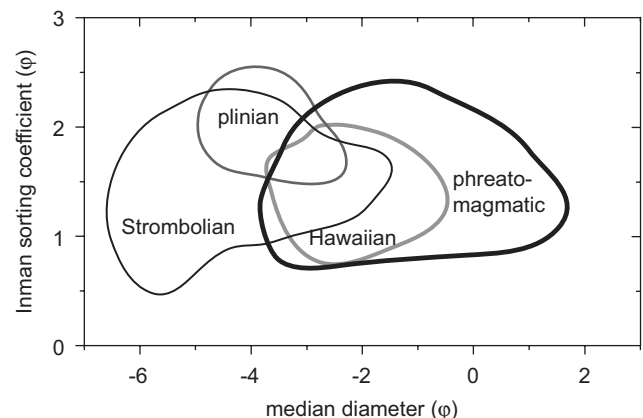


Fig. 14. Plot of medial diameter versus sorting coefficient for fall deposits from basaltic explosive eruptions modified after Walker and Croasdale (1972) and Houghton et al. (2000) to include Plinian data from Carey et al. (2007).

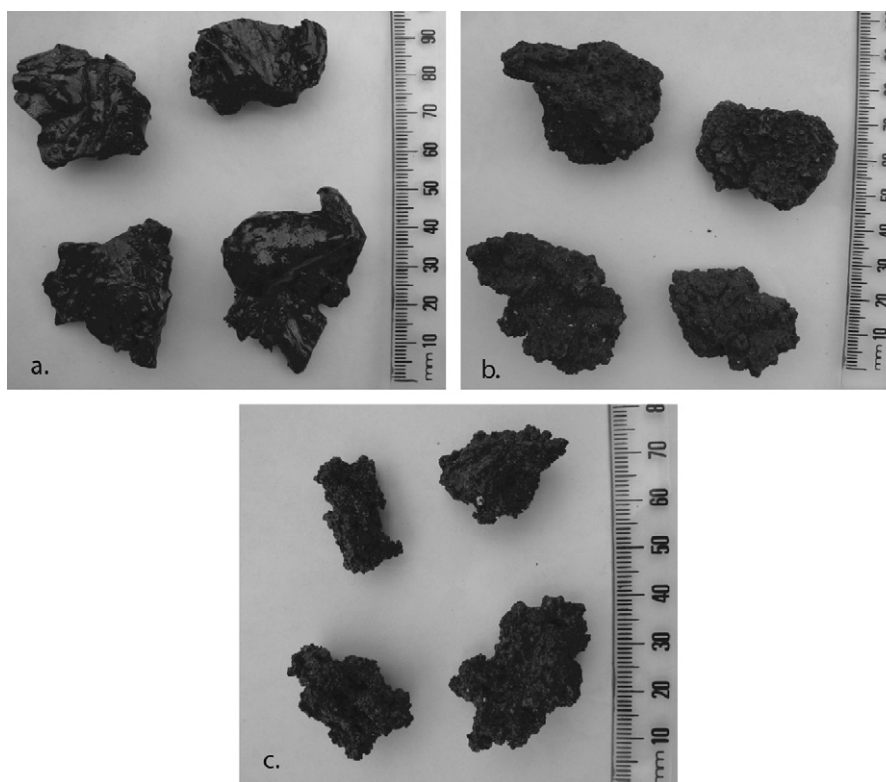


Fig. 15. Images of typical clast morphologies from (a) Hawaiian (Kīlauea Iki 1959, episode 1), (b) Strombolian (Stromboli 2002) and (c) basaltic Plinian (Tarawera 1886) eruptions. Note the highly fluidal nature of the former.

densities of $\sim 10^5$ to 10^6 cm^{-3} . An order-of-magnitude variation amongst pyroclasts in single samples (e.g., Lautze and Houghton, 2006) attests to the complexity of shallow processes of degassing and outgassing. Bubble and microlite textures in basaltic Plinian scoria contrast markedly with those in Strombolian and Hawaiian ejecta. Plinian clasts from the Etna 122 BC and Tarawera 1886 eruptions have relatively high vesicle number densities ($\sim 10^6$ to 10^8 cm^{-3}) and exceptionally high microlite crystallinities compared with these Hawaiian and Strombolian ejecta, typically 60–90% of the groundmass (Sable et al., 2006a, in press). The microlites also supply an efficient way of increasing the bulk viscosity of the magma to permit basaltic eruptions of Plinian intensity (Sable et al., in press). The complex 2001 and 2002–2003 eruptions of Etna, which included Strombolian and Hawaiian fountaining as well as phases of subplinian intensity, show a strong tie between explosion style and microlite content and vesicularity (Taddeucci et al., 2004a,b; Polacci et al., 2006). The proportion of microlite-poor and microlite-rich clasts at Etna reflects the dominant style of fragmentation and explosion (Taddeucci et al., 2002).

Many eruptions across the entire range of discharge rate show a progressive increase with time in the extent of outgassing of the melt (Taddeucci et al., 2002; Sable et al., 2006a), leading ultimately to the termination of explosive activity, via open-system outgassing.

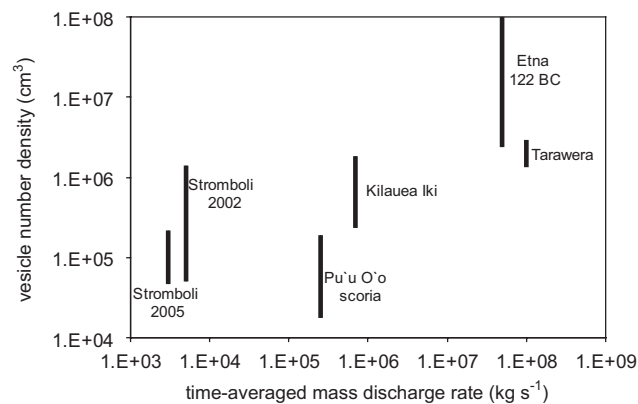


Fig. 16. Plot of range of vesicle number densities against time-averaged mass discharge rate for some historical basaltic eruptions. Data are as follows. Pu'u 'O'o: Cashman and Mangan (1994); Stromboli 2002: Lautze and Houghton (2005, 2006, 2007). Kīlauea Iki: our unpublished data. Stromboli 5 April 2003 paroxysm: Polacci et al. (2006); Etna 122 BC: Sable et al. (2006a). Tarawera: Sable et al. (in press).

4. Factors that control basaltic explosive dynamics

In this section we will discuss several primary, but interdependent, factors that ultimately control eruption dynamics. They are: (1) magma supply rate and volume;

(2) conduit geometry; (3) the abundance, style and depth of degassing of magmatic volatiles; (4) the fluid mechanics of magma ascent, including magma rheology; and (5) the mechanism and timing of magma break-up or fragmentation.

4.1. Magma supply

On time scales longer than, or equal to, eruptive episodes, changes in eruption intensity may be the manifestation of variations in magma supply from depth to the “shallow” magmatic plumbing system (e.g., Denlinger, 1997; Heliker et al., 1998; Garcia et al., 2000; Ripepe et al., 2005; Allard et al., 2006). For magma to erupt at the surface, sufficient excess pressure of magma within the source reservoir is required to overcome magmatic and dynamic pressure losses. Much of this excess pressure, or potential energy, is probably derived from volatiles (e.g., Pyle and Pyle, 1995; Vergnolle et al., 1996; Huppert and Woods, 2002). It is therefore likely that magma withdrawal, during eruptions and/or eruptive episodes, will result in pressure variations and, hence, variations in magma supply rate from shallow storage reservoirs to the conduit system and contrasts in eruption style (e.g., Taddeucci et al., 2004a; Ripepe et al., 2005; Allard et al., 2006). The ensuing dynamical coupling between magma source and conduit has been considered within various contexts for basaltic magmas (e.g., Vergnolle and Jaupart, 1986, 1989; Jaupart and Vergnolle, 1988; Vergnolle et al., 1996; Denlinger, 1997; Phillips and Woods, 2001; Meriaux and Jaupart, 1995; Ripepe et al., 2005; Pinel and Jaupart, 2004a, b; Woods et al., 2006).

Within the context of eruption styles, there is little doubt that a defining characteristic of Strombolian eruptions is the rapid and voluminous ascent of exsolved gas relative to a very low ascent rate of the melt phase (e.g., Wilson and Head, 1981; Braun and Ripepe, 1993; Vergnolle and Brandeis, 1994, 1996; Buckingham and Garces, 1996; Vergnolle et al., 1996, 2004; Ripepe and Gordeev, 1999; Ripepe et al., 2001; Chouet et al., 2003; Dubosclard et al., 2004; Gresta et al., 2004; Parfitt, 2004; Parfitt and Wilson, 1995, 1999; Patrick et al., 2007; Ripepe et al., 2005; Harris and Ripepe, 2007). In contrast, Hawaiian, subplinian and Plinian eruptions require a more sustained and higher rate of magma supply to the conduit system. However, given the apparent overlaps in discharge rate between individual eruption styles (Fig. 3), it is not clear to what extent other factors modulate, or maybe even control, transitions in eruptive style.

4.2. Conduit geometry

In the case of fissure eruptions (e.g., Thorarinsson et al., 1973; Self et al., 1974; Thordarson and Self, 1993;

Lockwood et al., 1987; Wilson and Head, 2001; Acocella et al., 2006; Carey et al., 2007; Hoskuldsson et al., 2007), the large cross-sectional area of the vent results in comparatively high discharge rates at relatively low magma ascent rates (Fig. 10). Conduit geometry may also play an important role in facilitating bubble accumulation, potentially of importance in Strombolian style eruptions (e.g., Ripepe and Gordeev, 1999; James et al., 2004, 2006; Menand and Phillips, 2007). However, because of the poor constraints on conduit geometry, little work has been done on detailed assessments of its effect on the dynamics of basaltic eruptions in general (e.g., Wilson, 1980; Wilson and Head, 2001; Mitchell, 2005).

4.3. Volatiles

Volatiles are important, because exsolved gases are less dense than the melt, but more compressible. The former imparts buoyancy, whereas the latter can be viewed as potential buoyancy or potential energy. Buoyancy from volatile exsolution ultimately allows magma to erupt (e.g., Parfitt et al., 1993; Pyle and Pyle, 1995; Woods and Cardoso, 1997). There are four processes whereby magma gains buoyancy: (1) ascent-driven decompression lowers volatile solubility, resulting in volatile exsolution and bubble growth (e.g., Sparks, 1978; Proussevitch et al., 1993; Gonnermann and Manga, 2007); (2) crystallization enriches the melt fraction in volatiles, resulting in volatile exsolution (e.g., Carmichael et al., 1974; Tait et al., 1989); (3) ascent-driven decompression results in volume expansion of exsolved volatiles (e.g., Sparks, 1978; Proussevitch et al., 1993); and (4) buoyantly ascending decoupled bubbles may rise and/or accumulate elsewhere in the conduit system (e.g., Wilson, 1980; Wilson and Head, 1981; Vergnolle and Jaupart, 1986, 1990; Jaupart and Vergnolle, 1988, 1989; Parfitt, 2004; Parfitt and Wilson, 1995; Parfitt et al., 1995; James et al., 2004; Menand and Phillips, 2007).

Aside from the fluid dynamics of gas–liquid flows, volatiles may affect eruptive behavior of basalt magmas through (1) closed-system ascent of melt and bubbles resulting in rapid decompressive bubble growth or build-up of overpressure and ultimately magma fragmentation (e.g., Alidibirov and Dingwell, 1996; Zimanski et al., 1997; Zhang, 1999; Spieler et al., 2004; Gonnermann and Manga, 2007; Namiki and Manga, 2008); (2) feedbacks between volatile exsolution, decompression, magma crystallization and magma rheology (e.g., Sparks and Pinkerton, 1978; Metrich and Rutherford, 1998; Metrich et al., 2001; Del Carlo and Pompilio, 2004; Simakin and Salova, 2004); (3) open-system gas loss at depth leaving a relatively volatile-depleted magma with decreased potential for explosivity (e.g.,

Vergnolle et al., 1996; Roggensack et al., 1997; Clarke et al., 2002, 2007; Melnik and Sparks, 2002; Melnik et al., 2005); (4) open-system accumulation of volatiles (e.g., Andronico et al., 2005; Allard et al., 2006; Burton et al., 2007; Menand and Phillips, 2007; D'Alessandro et al., 1997), possibly resulting in the formation of gas slugs and Strombolian style eruptions (e.g., Jaupart and Vergnolle, 1989; Allard et al., 1991; Burton et al., 2007; Menand and Phillips, 2007); and (5) development of permeable pathways allowing for open-system gas loss and decrease in explosivity (e.g., Eichelberger et al., 1986; Stasiuk et al., 1996; Melnik and Sparks, 2002; Melnik et al., 2005; Ida, 2007; Namiki and Manga, 2008; Polacci et al., 2008).

The relative importance of pre-eruptive volatile content versus syn-eruptive loss of volatiles is a key question to understanding the dynamics of explosive basaltic eruptions (Roggensack et al., 1997; Del Carlo and Pompilio, 2004). However, to what extent systematic variations in pre-eruptive volatile content correlate with eruptive behavior remains largely unexplored within the broader context of eruption dynamics or explosivity. The two most abundant volatiles in basaltic magmas are H₂O and CO₂ (e.g., Johnson et al., 1994; Dixon and Stolper, 1995; Dixon et al., 1995, 1997; Schmincke, 2004; Papale, 2005; Wallace, 2005). Volatile solubility in silicate melts is primarily pressure dependent, with secondary dependence on temperature and on melt composition, including other volatile species (e.g., McMillan, 1994; Blank and Brooker, 1994; Dixon et al., 1997; Newman and Lowenstern, 2002; Papale et al., 2006). Basaltic magmas show a wide range of water contents ranging from <0.5 to 6–8 wt% (e.g., Sisson and Grove, 1993; Johnson et al., 1994; Wallace, 2005), with non-arc basalts generally being considerably drier (e.g., Kīlauea up to 1 wt%, Wallace and Anderson, 1998; Gerlach et al., 2002; Hauri, 2002) than arc magmas (up to ca. 4 wt% at Etna, e.g., Metrich et al., 2004; Spilliaert et al., 2006a, b; Kamenetsky et al., 2007; up to 3.4 wt% at Stromboli, Metrich et al., 2005), where water content can be highly variable. CO₂ content is more difficult to constrain, because low CO₂ solubility results in glasses and melt inclusions with lower CO₂ concentrations than the parental magma. Measured H₂O and CO₂ in melt inclusions in conjunction with H₂O–CO₂ solubility relations suggests that arc magmas also contained several wt% of CO₂, much of which exsolved pre-eruptively during vapor-saturated fractional crystallization (e.g., Papale, 2005; Wallace, 2005; Wade et al., 2006). Thus, magmas may already contain, or have lost, significant amounts of volatile bubbles prior to eruption. Overall, CO₂ solubility is lower than that of H₂O so that CO₂ will exsolve at greater depths (pressures) than H₂O. Consequently, relative proportions of CO₂ and H₂O in erupted gases, or in glasses and melt inclusions, can provide constraints on depths of

magma degassing (Burton et al., 2007; Edmonds and Gerlach, 2007). S, Cl and F are also present in volcanic gases at measurable quantities. Because S is less soluble than Cl, which in turn is less soluble than F (Carroll and Webster, 1994), these gases have also been used to constrain degassing depth and style. Recent successful applications have, for example, been to Etna (Metrich et al., 2004; Allard et al., 2005; Spilliaert et al., 2006a, b), Stromboli (Burton et al., 2007) and Kīlauea (Edmonds and Gerlach, 2007).

4.4. Fluid mechanics of magma ascent

4.4.1. General considerations

Exsolving volatiles in ascending magmas form bubbles, which are always buoyant relative to the surrounding melt. Bubble rise depends primarily on size, volume fraction and melt viscosity (e.g., Batchelor, 1967). Bubble size and volume fraction are expected to increase during ascent due to continued volatile exsolution, decompression and coalescence (e.g., Sparks, 1978), which by themselves may affect flow dynamics (e.g., Cheng et al., 2002). At the same time, viscosity may increase due to the loss of dissolved volatiles, decrease in temperature and crystallization (e.g., Gonnermann and Manga, 2007 and references therein), which in turn will affect bubble rise velocities.

On eruptive time scales mass discharge rate depends on the total pressure drop between magma reservoir and the surface. Locally within the conduit the pressure gradient is, to first order, the sum of the contributions due to gravity and friction (e.g., Guet and Ooms, 2006). The gravitational part depends on the density of the gas–liquid mixture, which is predominantly controlled by the bubble volume fraction. The frictional pressure gradient can, to first order, be estimated on the basis of established single-phase flow correlations (e.g., Wilson, 1980; Wilson and Head, 1981; Koyaguchi, 2005; Guet and Ooms, 2006). Over a wide range of flow conditions, the frictional pressure gradient is dominant for liquid–gas flows in vertical columns (e.g., Guet and Ooms, 2006), implying for magmatic systems that vesicularity has a significant influence on global flow conditions.

Wilson (1980), Wilson and Head (1981), Parfitt and Wilson (1995), Parfitt et al. (1995) and Parfitt (2004) suggested that major transitions in explosive eruption of basaltic magmas are the consequence of the degree to which bubbles and the melt phase are coupled, a function of viscosity, bubble size and abundance, as well as discharge/ascent rate. In the fluid dynamics community, it has long been known that small perturbations in gas–liquid flow systems can lead to huge oscillations in flow rates and flow regimes (e.g., Baker, 1954; Taitel et al., 1980; Tutu, 1982, 1984; Furukawa and Fukano, 2001; Cheng et al., 2002; Hibiki

and Ishii, 2003a, b; McNeil and Stuart, 2003, 2004; Hu and Golan, 2004; Guet and Ooms, 2006; Guet et al., 2006; Ornebere-Iyari et al., 2007). The most sensitive parameters in controlling perturbations or transitions in flow dynamics are probably the rate and nature of gas flux. For magmas it should be expected that rheology, because of its large variability, can play an additional important role. Bubble mobility scales inversely with liquid viscosity and is likely to affect the overall fluid dynamics of the flow. In the engineering literature, the fluid dynamics of bubbly flows has received considerable attention and four basic flow regimes have been identified: bubble flow, slug flow, churn flow and annular flow (Fig. 17). While these flow regimes occur over a wide range of conditions, inconsistencies and open questions remain, especially in terms of applicability to basaltic eruptions, where length scales, viscosities and pressures exceed the conditions of most experimental investigations. Nonetheless, the general principles of gas–liquid flows should be instructive for the understanding of magmatic systems.

4.4.2. Strombolian style eruptions

For gas–liquid flow in vertical columns with low gas flow rates and small bubbles relative to the conduit diameter, bubbles are more or less randomly dispersed and move upward through the liquid phase without much dynamical interaction. This is called the bubble flow regime (Fig. 17). At higher gas flow rates, bubble number density is no longer uniformly distributed and hydrodynamic interactions can potentially affect the dynamics along the entire length of the conduit system. Originally it was thought that collisions between bubbles result in coalescence and ultimately to large bubbles of

comparable size to the diameter of the conduit (Radovcich and Moissis, 1962). These are generally referred to as gas slugs, or Taylor bubbles, and the associated flow regime is called cap or slug flow (Fig. 17). A consequence of this hypothesis was that, given a sufficiently long residence time within the conduit, bubble flow should invariably pass to slug flow. Subsequently, it was suggested that dispersed bubble flow could be maintained if there is sufficient bubble break-up due to liquid turbulence to balance bubble coalescence (Taitel et al., 1980). More recently it was found that the transition to slug flow occurs simultaneously throughout the liquid column, implying that bubble coalescence and break-up are not the underlying mechanisms responsible for this flow transition (Hewitt, 1990). Instead, the bubble-to-slug transition may be associated with instabilities of void-fraction waves, or bubble clusters, that form dynamically within the flow (e.g., Wallis, 1969; Saiz-Jabardo and Bouré, 1989; Park et al., 1993; Cheng et al., 1998). In some conditions, bubble flow passes directly to churn flow (Cheng et al., 1998), which typically occurs at higher gas flow rates than slug flow (Fig. 17). Void-fraction time series from laboratory experiments of slug and cap flow (e.g., Cantelli et al., 2006) are suggestive of Strombolian eruptions, at least in some cases, being the consequence of analogous fluid-dynamical regimes within the conduit producing an intermittently high rate of gas flux. In fact, it has been suggested that at low magma ascent rates bubbles and melt become decoupled, resulting in open-system degassing (e.g., Wilson and Head, 1981; Parfitt, 2004; Parfitt and Wilson, 1995; Parfitt et al., 1995). Bubbles rise relative to the melt phase leaving a relatively volatile-depleted magma with lowered explosive potential (Taddeucci et al., 2002). Dynamical interaction between bubbles may result in significant bubble coalescence (e.g., Wilson and Head, 1981; Parfitt, 2004; Parfitt and Wilson, 1995; Parfitt et al., 1995) or bubble accumulation (e.g., Allard, 2007; Edmonds and Gerlach, 2007) thought to be required processes for Strombolian style eruptions.

Both processes may be enhanced or facilitated at geometric asperities within the magmatic plumbing system where bubbles can accumulate (e.g., James et al., 2004).

4.4.3. Hawaiian style eruptions

Churn flow (Fig. 17) occurs at higher gas flow rates than slug flow. Unlike slug flow, it is characterized by neither phase being continuous, and by highly unsteady behavior (e.g., Cantelli et al., 2006). At gas flow rates that are at least 10 times larger than liquid flow rates, churn flow passes to annular flow, where the gas phase essentially occupies almost the entire conduit and is surrounded by a relatively thin annulus of liquid along the conduit walls. Both churn and annular flow produce

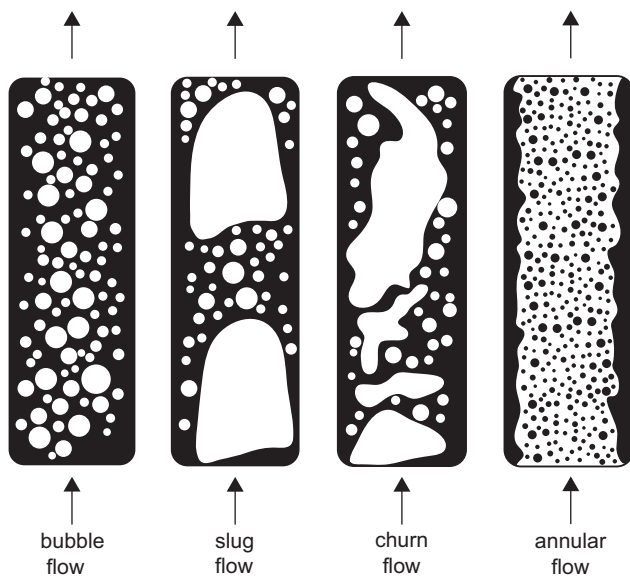


Fig. 17. Flow regimes for vertically rising bubbly liquids after Taitel et al. (1980) and Guet and Ooms (2006).

more sustained and vigorous flow conditions than slug flow. For churn and annular flow, the gas phase is continuous, albeit heterogeneously and somewhat intermittently, on length scales that approach the diameter of the conduit. It has been suggested that magma flow in the volcanic conduit during Hawaiian style eruptions is associated with annular flow (Vergnolle and Jaupart, 1986, 1990; Jaupart and Vergnolle, 1988, 1989), where it is assumed that annular flow is the consequence of bubble accumulation and coalescence at the roof of a shallow magma storage reservoir. More or less continuous collapse of this “foam” is then thought to give rise to a relatively continuous, high gas flux into the conduit system, capable of sustaining Hawaiian style magma jets for durations of hours.

In contrast, Wilson (1980), Wilson and Head (1981), Parfitt and Wilson (1995), Parfitt et al., 1995) and Parfitt (2004) suggest that for small bubbles and/or high magma ascent rates bubbles are unable to move appreciably relative to the melt phase, i.e., melt and bubbles are coupled. Consequently, the gas phase is dispersed throughout the magma producing a highly vesicular magma with relatively small bubbles. At some point the magma “disrupts” or “fragments”.

4.4.4. Subplinian and Plinian basaltic eruptions

What governs the transition to subplinian or Plinian eruptive styles remains largely unresolved. Recently it has been suggested that subplinian activity at Shishaldin volcano, Alaska in 1999 was the consequence of bubble accumulation, coalescence and collapse beneath the roof of a shallow magma reservoir (Vergnolle and Caplan-Auerbach, 2006). This would suggest that the observed subplinian activity is simply a more intense form of Strombolian or Hawaiian style eruptions. The latter is not inconsistent with results from an analysis of tephra dispersal from the Hawaiian style 1959 Kīlauea Iki eruption of Kīlauea volcano, Hawai‘i. Here it was concluded that Hawaiian eruptions are dynamically indistinguishable from Plinian eruptions (Parfitt, 1998; Parfitt and Wilson, 1999).

This, however, contradicts the general view that Plinian style eruptions are associated with brittle magma fragmentation (e.g., Cioni et al., 2000), as low viscosity basalt cannot fragment in a truly brittle manner at discharge rates typical for Hawaiian style eruptions (e.g., Namiki and Manga, 2008). It therefore remains unclear to what extent models derived from tephra dispersal studies can be reconciled with constraints on magma fragmentation processes (e.g., Zimanowski et al., 1997; Spieler et al., 2004; Taddeucci et al., 2004b; Namiki and Manga, 2008). Based on textural observations of tephra from subplinian and Plinian basaltic eruptions, it has been suggested that basaltic subplinian and Plinian eruptions are distinct from Hawaiian style eruptions and may be the consequence

of brittle fragmentation of microlite-rich magma (e.g., Taddeucci et al., 2004a, b; Sable et al., 2006a; Gonnermann et al., in press). This hypothesis is based on the rheological stiffening of the microlite-rich melt phase leading to sufficient gas overpressure for brittle magma fragmentation during rapid, ascent-driven decompression (Gonnermann et al., in press).

4.5. Magma fragmentation

Within realistic ranges of compositional variability, eruptive temperatures and volatile content, viscosity of crystal- and vesicle-free basalt liquids may vary by up to two orders of magnitude (e.g., Giordano and Dingwell, 2003; Hui and Zhang, 2007). The bulk viscosity of bubbly magma varies significantly as the volume fraction of bubbles increases (e.g., Lejeune et al., 1999; Manga and Loewenberg, 2001; Llewellyn et al., 2002; Pal, 2003, 2004; Llewellyn and Manga, 2005; Gonnermann and Manga, 2007). Moreover, the presence of crystals or microlites, which may reach up to 90% in some basalt magmas (e.g., Sable et al., 2006a), will significantly increase magma viscosity (Lejeune and Richet, 1995; Stevenson et al., 1996; Saar et al., 2001; Pal, 2002; Deubener, 2003; Costa, 2005; Arbaret et al., 2007; Caricchi et al., 2007; Gonnermann and Manga, 2007; Lavalley et al., 2007). It can therefore be concluded that the rheological effects of bubbles and crystallinity are important potential factors modulating eruption dynamics.

Rheological stiffening of magma results in increased dynamic pressure loss and inability of bubbles to expand upon decompression. While the mechanism by which the basalt magma becomes fragmented may differ between eruption styles and in general remains somewhat controversial (e.g., Sparks et al., 1994; Parfitt, 1998; Wilson, 1999; Spieler et al., 2004; Taddeucci et al., 2004b; Namiki and Manga, 2005, 2008), there is little doubt that decompression rate is a key factor. Conventionally, it had been assumed that fragmentation occurs at a critical volume fraction of bubbles, presumably due to the instability of thin bubble walls (e.g., Verhoogen, 1951; Sparks, 1978; Wilson and Head, 1983; Parfitt and Wilson, 1995). At present, the two commonly invoked “brittle” fragmentation mechanisms are “strain-rate dependent” (Webb and Dingwell, 1990; Dingwell, 1996; Papale, 1999) and “stress dependent” (McBirney and Murase, 1970; Alidibirov, 1994; Zhang, 1999; Spieler et al., 2004) fragmentation. Basalt magma, if it is relatively poor in crystals and microlites, is not expected to undergo brittle fragmentation (e.g., Papale, 1999), but instead may fragment via “inertial fragmentation”, where the expansion of gas bubbles during decompression results in inertial stretching and breakup of the liquid magma (e.g., Shimozuru, 1994;

Zimanowski et al., 1997; Namiki and Manga, 2008; Villermaux, 2007; Eggers and Villermaux, 2008). This is consistent with the abundant presence of fluidal textures (Fig. 15) in clasts derived from Hawaiian style eruptions (e.g., Heiken and Wohletz, 1985). However, in the presence of abundant microlites and/or crystals, the effective viscosity of the melt+solids suspension is expected to increase by orders of magnitude, relative to the melt phase. Consequently, decompressive bubble growth may be viscously retarded leading to sufficient built-up of overpressure for brittle magma fragmentation. Thus, if magma source conditions are sufficient for sustained eruptive episodes, brittle fragmentation of microlite-rich basalt magma may result in subplinian or Plinian eruptions (e.g., Taddeucci et al., 2004a, b; Sable et al., 2006a; Gonnermann et al., in press).

Hawaiian, subplinian and Plinian eruptions are characterized by sustained, high magma discharge rates, but differing mechanisms by which magma with micrometer- to centimeter-size bubbles fragments. In contrast, during Strombolian eruptions it appears to be the fluid dynamics by which single meter-size bubbles, or perhaps clusters of large bubbles, rupture at the magma surface that results in the break-up and ejection of melt that surrounds these gas slugs (e.g., Blackburn et al., 1976; Wilson, 1980).

5. Discussion and conclusions

5.1. Steadiness in basaltic explosive volcanism

A simple way to view the contrast between Hawaiian and Plinian versus Strombolian explosivity is that the former are “steady”, with sustained discharge on time scales of hours to (rarely) days (e.g., Chouet et al., 1973; Ripepe et al., 1993; Patrick et al., 2007) as a consequence of sufficient magma flux and more or less closed-system degassing, whereas the latter are a sequence of discrete impulsive events lasting typically seconds to (rarely) minutes (Richter et al., 1970; Walker et al., 1984; Heliker et al., 2003) involving open-system behavior and low magma flux.

In practice even Hawaiian fountaining is characterized by major fluctuations in exit velocity and mass flux (Figs. 9 and 11). Exit velocity in Hawaiian eruptions scales approximately with the square root of fountain height, and the data in Figs. 9 and 11 suggest height variations of at least an order of magnitude on time scales of minutes. Explaining this variability is an important second order problem, perhaps the most significant one, for models of magma and gas transport in the shallow conduit at Kīlauea.

We have no direct evidence for the extent of unsteadiness in basaltic Plinian eruptions; however, the

complex pattern of proximal sedimentation in the 1886 Tarawera eruption with at places more than 50 distinct beds formed over a 5-h time window (Sable et al., 2006b; Carey et al., 2007) points to both abrupt and phased, reversible changes in mass discharge rate and exit velocity.

Much of this diversity in basaltic explosive eruptions relates to the ease with which bubbles nucleate and mature in fluid basaltic melts with respect to silicic magmas where viscous effects are much more significant. In basaltic systems, degrees of volatile supersaturation are generally much lower leading to lower bubble number densities (Fig. 16), but the depth interval of bubble nucleation is probably much wider and bubbles decouple from the melt phase over a considerable depth interval (Spilliaert et al., 2006a, b; Burton et al., 2007; Edmonds and Herd, 2007).

5.2. Conclusions

Basaltic explosive eruptions span a range of six orders of magnitude in mass discharge rate (10^2 to 10^8 kg s⁻¹) and include examples of Strombolian, Hawaiian, subplinian and Plinian explosivity. There is no simple correlation between these eruptive styles and average mass flux. Additionally, single eruptions will contain events of two or more types and pass rapidly from Strombolian to Hawaiian or Strombolian to subplinian and vice versa. Long-lived Hawaiian eruptions often will include examples of brief spattering explosions more similar to Strombolian explosions, whereas the high frequency of Strombolian explosions at Etna and elsewhere defines a transition towards steady-state behavior, perhaps equivalent to Hawaiian fountaining.

Eruptive style is most strongly influenced by magma supply rate and degassing and the extent of coupling of gas and melt phases prior to and during ascent. Feedbacks between ascent rate, syn-eruptive microlite growth, magma rheology and fragmentation, as well as bubble growth, mobility and coalescence, define a complex dynamical system with an inherent propensity toward nonlinear behavior that may manifest itself through abrupt shifts in eruption style.

Acknowledgements

We thank Associate Editor Klaus Keil for soliciting this Invited Review. This paper draws on intense field work conducted at five basaltic volcanoes and the input and insight of the following colleagues – Kīlauea: Sarah Fagents, Don Swanson, Wendy Stovall. Stromboli: Andy Harris, Nicole Lautze, Matt Patrick, Maurizio Ripepe. Tarawera: Rebecca Carey, Armin Freundt, Julia Sable, Colin Wilson. Etna: Danielle Andronico,

Mauro Coltelli, Paola Del Carlo, Jim Gardner, Simone Scollo, Jacopo Taddeucci. Masaya: Costanza Bonadonna, Licia Costantini. The paper was improved greatly by reviews from Klaus Keil and Lionel Wilson and art work by Penny Larin. The research was supported by the following NSF awards: EAR-0125719 and EAR-0537459.

References

- Acocella, V., Neri, M., Scarlato, P., 2006. Understanding shallow magma emplacement at volcanoes: orthogonal feeder dikes during the 2002–2003 Stromboli (Italy) eruption. *Geophys. Res. Lett.* 33.
- Alidibirov, M., 1994. A model for viscous magma fragmentation during volcanic blasts. *Bull. Volcanol.* 56, 459–465.
- Alidibirov, M., Dingwell, D.B., 1996. Magma fragmentation by rapid decompression. *Nature* 380, 146–148.
- Allard, P., 2007. A CO₂-rich gas trigger of explosive paroxysms at Stromboli volcano (Italy). *Geophys. Res. Abs.* 9, 2.
- Allard, P., Carbonnelle, J., Dajlevic, D., Lebronec, J., Morel, P., Robe, M.C., Maurenas, J.M., Faivrepietret, R., Martin, D., Sabroux, J.C., Zettwoog, P., 1991. Eruptive and diffuse emissions of CO₂ from Mount Etna. *Nature* 351, 387–391.
- Allard, P., Carbonnelle, J., Metrich, N., Loyer, H., Zettwoog, P., 1994. Sulphur output and magma degassing budget of Stromboli volcano. *Nature* 368, 326–330.
- Allard, P., Burton, M., Mure, F., 2005. Spectroscopic evidence for a lava fountain driven by previously accumulated magmatic gas. *Nature* 433, 407–410.
- Allard, P., Behncke, B., D'Amico, S., Neri, M., Gambino, S., 2006. Mount Etna 1993–2005: anatomy of an evolving eruptive cycle. *Earth Sci. Rev.* 78, 85–114.
- Alparone, S., Andronico, D., Sgroi, T., Ferrari, F., Lodato, L., Reitano, D., 2007. Alert system to mitigate tephra fallout hazards at Mt. Etna Volcano, Italy. *Nat. Hazards* 18.
- Andronico, D., Branca, S., Calvari, S., Burton, M., Caltabiano, T., Corsaro, R.A., Miraglia, L., Mure, F., Neri, M., Pecora, E., Pompilio, M., Salerno, G., Spampinato, L., 2005. A multi-disciplinary study of the 2002–03 Etna eruption: insights into a complex plumbing system. *Bull. Volcanol.* 67, 314–330.
- Andronico, D., Cristaldi, A., Taddeucci, A., 2007. Eruzione Stromboli 2007-L'evento parossistico del 15 marzo. Istituto Nazionale di Geofisica e Vulcanologia Internal Report UFGV-2007-016.
- Arbaret, L., Bystricky, M., Champallier, R., 2007. Microstructures and rheology of hydrous synthetic magmatic suspensions deformed in torsion at high pressure. *J. Geophys. Res.* 112, B10208.
- Baker, O., 1954. Simultaneous flow of oil and gas. *Oil Gas J.* 53, 185–190.
- Barberi, F., Rosi, M., Sodi, A., 1993. Volcanic hazard assessment at Stromboli based on review of historical data. *Acta Vulcanol.* 3, 173–187.
- Batchelor, G.K., 1967. *An Introduction to Fluid Dynamics*. Cambridge University Press, p. 615.
- Behncke, B., Neri, M., Pecora, E., Zanon, V., 2006. The exceptional activity and growth of the Southeast Crater, Mount Etna (Italy), between 1996 and 2001. *Bull. Volcanol.* 69, 149–173.
- Bice, D.C., 1985. Quaternary volcanic stratigraphy of Managua, Nicaragua: correlation and source assignment for multiple overlapping plinian deposits. *Geol. Soc. Am. Bull.* 96, 553–566.
- Blackburn, E.A., Wilson, L., Sparks, R.S.J., 1976. Mechanisms and dynamics of strombolian activity. *J. Geol. Soc., Lond.* 132, 429–440.
- Blank, J.G., Brooker, R.A., 1994. Experimental studies of carbon-dioxide in silicate melts – solubility, speciation, and stable carbon-isotope behavior, volatiles in magmas. *Rev. Min.* 30, 157–186.
- Bonaccorso, A., 2006. Explosive activity at Mt. Etna summit craters and source modeling by using high-precision continuous tilt. *J. Volcanol. Geotherm. Res.* 158, 221–234.
- Bonadonna, C., Houghton, B.F., 2005. Total grain-size distribution and volume of tephra-fall deposits. *Bull. Volcanol.* 67, 441–456.
- Bonadonna, C., Ernst, G.G.J., Sparks, R.S.J., 1998. Thickness variations and volume estimates of tephra fall deposits: the importance of particle Reynolds number. *J. Volcanol. Geotherm. Res.* 81, 173–187.
- Bonadonna, C., Phillips, J.C., Houghton, B.F., 2005. Modeling tephra sedimentation from a Ruapehu weak plume eruption. *J. Geophys. Res.* 110, B08209.
- Branca, S., del Carlo, P., 2005. Types of eruptions of Etna volcano AD 1670–2003: implications for short-term eruptive behaviour. *Bull. Volcanol.* 67, 732–742.
- Braun, T., Ripepe, M., 1993. Interaction of seismic and air waves recorded at Stromboli Volcano. *Geophys. Res. Lett.* 20, 65–68.
- Buckingham, M.J., Garces, M.A., 1996. Canonical model of volcano acoustics. *J. Geophys. Res.* 101, 8129–8151.
- Burton, M., Allard, P., Mure, F., La Spina, A., 2007. Magmatic gas composition reveals the source depth of slug-driven Strombolian explosive activity. *Science* 317, 227–230.
- Calvari, S., Spampinato, L., Lodato, L., 2005. The 5 April 2003 vulcanian paroxysmal explosion at Stromboli volcano (Italy) from field observations and thermal data. *J. Volcanol. Geotherm. Res.* 149, 160–175.
- Cantelli, L., Fichera, A., Guglielmino, I.D., Pagano, A., 2006. Nonlinear dynamics of air–water mixtures in vertical pipes: experimental trends. *Int. J. Bifur. Chaos* 16, 2749–2760.
- Carey, S., Sparks, R.S.J., 1986. Quantitative models of fallout and dispersal of tephra from volcanic eruption columns. *Bull. Volcanol.* 48, 109–125.
- Carey, R.J., Houghton, B.F., Sable, J.E., Wilson, C.J.N., 2007. Contrasting grain size and componentry in complex proximal deposits of the 1886 Tarawera basaltic plinian eruption. *Bull. Volcanol.* 69, 903–926.
- Caricchi, L., Burlini, L., Ulmer, P., Gerya, T., Vassalli, M., Papale, P., 2007. Non-Newtonian rheology of crystal-bearing magmas and implications for magma ascent dynamics. *Earth Planet. Sci. Lett.* 264, 402–419.
- Carmichael, I., Turner, F., Verhoogen, J., 1974. *Igneous Petrology*. McGraw-Hill Book Co., New York, p. 739.

- Carroll, M.R., Webster, J.D., 1994. Solubilities of sulfur, noble-gases, nitrogen, chlorine, and fluorine in magmas. In: *Volatiles in Magmas*. *Rev. Min.* 30, 231–279.
- Carveni, P., Romano, R., Caltabiano, T., Grasso, M.F., Gresta, S., 1994. The exceptional explosive activity of 5 January 1990 at the SE-Crater of Mt. Etna Volcano (Sicily). *Boll. Soc. Geol.* 113, 613–631.
- Cashman, K.V., Mangan, M.T., 1994. Physical aspects of magmatic degassing. II. Constraints on vesiculation processes from textural studies of eruptive products. In: Carroll, M.R., Holloway, J.R. (Eds.), *Volatiles in Magmas*. *Rev. Min.* 30, 447–478.
- Cheng, H., Hills, J.H., Azzorparadi, B.J., 1998. A study of the bubble-to-slug transition in vertical gas–liquid flow in columns of different diameter. *Int. J. Multiphase Flow* 24, 431–452.
- Cheng, H., Hills, J.H., Azzorparadi, B.J., 2002. Effects of initial bubble size on flow pattern transition in a 28.9 mm diameter column. *Int. J. Multiphase Flow* 28, 1047–1062.
- Chouet, B., Hamisevicz, N., McGetchin, T.R., 1973. Photoballistics of volcanic jet activity at Stromboli, Italy. *J. Geophys. Res.* 79, 4961–4976.
- Chouet, B., Saccorotti, G., Dawson, P., Martini, M., Scarpa, R., Deluca, G., Milana, G., Cattaneo, M., 1999. Broadband measurements of the sources of explosions at Stromboli Volcano, Italy. *Geophys. Res. Lett.* 26, 1937–1940.
- Chouet, B., Dawson, P., Ohminato, T., Martini, M., Saccorotti, G., Giudicepietro, F., De Luca, G., Milana, G., Scarpa, R., 2003. Source mechanisms of explosions at Stromboli Volcano, Italy, determined from moment-tensor inversions of very-long-period data. *J. Geophys. Res.* 108.
- Cioni, R., Marianelli, P., Santacroce, R., Sbrana, A., 2000. Plinian and Subplinian eruptions. In: Sigurdsson, H. (Ed.), *Encyclopedia of Volcanoes*. Academic Press, San Diego, CA, pp. 477–494.
- Clarke, A.B., Voight, B., Neri, A., Macedonio, G., 2002. Transient dynamics of vulcanian explosions and column collapse. *Nature* 415, 897–901.
- Clarke, A.B., Stephens, S., Teasdale, R., Sparks, R.S.J., Diller, K., 2007. Petrologic constraints on the decompression history of magma prior to Vulcanian explosions at the Soufriere Hills volcano, Montserrat. *J. Volcanol. Geotherm. Res.* 161, 261–274.
- Cole, P.D., Fernandez, E., Duarte, E., Duncan, A.M., 2005. Explosive activity and generation mechanisms of pyroclastic flows at Arenal volcano, Costa Rica between 1987 and 2001. *Bull. Volcanol.* 67, 695–716.
- Coltelli, M., Del Carlo, P., Vezzoli, L., 1998. Discovery of a Plinian basaltic eruption of Roman age at Etna volcano, Italy. *Geology* 26, 1095–1098.
- Coltelli, M., Del Carlo, P., Vezzoli, L., 2000. Stratigraphic constraints for explosive activity in the past 100 ka at Etna Volcano, Italy. *Int. J. Earth Sci.* 89, 665–677.
- Corsaro, R.A., Miraglia, L., 2005. Dynamics of 2004–2005 Mt. Etna effusive eruption as inferred from petrologic monitoring. *Geophys. Res. Lett.* 32, L13302.
- Costa, A., 2005. Viscosity of high crystal content melts: dependence on solid fraction. *Geophys. Res. Lett.* 32.
- Costantini, L., Bonadonna, C., Houghton, B.F., Wehrmann, H. Basaltic Plinian volcanism: new perspectives on the Fontana Lapilli eruption, Nicaragua. *J. Volcanol. Geotherm. Res.*, in press.
- D'alessandro, W., Giammanco, S., Parello, F., Valenza, M., 1997. CO₂ output and delta C-13(CO₂) from Mount Etna as indicators of degassing of shallow asthenosphere. *Bull. Volcanol.* 58, 455–458.
- Del Carlo, P., Pompilio, M., 2004. The relationship between volatile content and the eruptive style of basaltic magma: the Etna case. *Ann. Geophys.* 47, 1423–1432.
- Denlinger, R.P., 1997. A dynamic balance between magma supply and eruption rate at Kilauea volcano, Hawaii. *J. Geophys. Res.* 102, 18091–18100.
- Deubener, J., 2003. Flow of partially crystallised silicate melts. *Glass Sci. Technol.* 76, 20–25.
- Dingwell, D.B., 1996. Volcanic dilemma: flow or blow? *Science* 273, 1054–1055.
- Dixon, J.E., Stolper, M., 1995. An experimental study of water and carbon dioxide solubilities in mid-ocean ridge basaltic liquids. 2: Applications to degassing. *J. Pet.* 36, 1633–1646.
- Dixon, J.E., Stolper, M., Holloway, J.R., 1995. An experimental study of water and carbon dioxide solubilities in mid ocean ridge basaltic liquids. 1: Calibration and solubility models. *J. Pet.* 36, 1607–1631.
- Dixon, J.E., Clague, D.A., Wallace, P., Poreda, R., 1997. Volatiles in alkalic basalts from the North Arch volcanic field, Hawaii: extensive degassing of deep submarine-erupted alkalic series lavas. *J. Pet.* 38, 911–939.
- Dubosclard, G., Donnadiou, F., Allard, P., Cordesses, R., Hervier, C., Coltelli, M., Privitera, E., Kornprobst, J., 2004. Doppler radar sounding of volcanic eruption dynamics at Mount Etna. *Bull. Volcanol.* 66, 443–456.
- Duffield, W.A., Christiansen, R.L., Koyanagi, R., Peterson, D.W., 1982. Storage, migration, and eruption of magma at Kilauea volcano, Hawaii, 1971–1972. *J. Volcanol. Geotherm. Res.* 13, 273–307.
- Edmonds, M., Gerlach, T.M., 2007. Vapor segregation and loss in basaltic melts. *Geology* 35, 751–754.
- Edmonds, M., Herd, R.A., 2007. A volcanic degassing event at the explosive-effusive transition. *Geophys. Res. Lett.* 34, L21310, doi:10.1029/2007GL031379.
- Eggers, J., Villermaux, E., 2008. Physics of liquid jets. *Rep. Prog. Phys.* 71, 79.
- Eichelberger, J.C., Carrigan, C.R., Westrich, H.R., Price, R.H., 1986. Non-explosive silicic volcanism. *Nature* 323, 598–602, 10.1038/323598a0.
- Furukawa, T., Fukano, T., 2001. Effects of liquid viscosity on flow patterns in vertical upward gas–liquid two-phase flow. *Int. J. Multiphase Flow* 27, 1109–1126.
- Garcia, M.O., Rhodes, J.M., Wolfe, E.W., Ulrich, G.E., Ho, R.A., 1992. Petrology of lavas from episodes 2–47 of the Puu Oo eruption of Kilauea volcano, Hawaii: evaluation of magmatic processes. *Bull. Volcanol.* 55, 1–16.
- Garcia, M.O., Pietruszka, A.J., Rhodes, J.M., Swanson, K., 2000. Magmatic processes during the prolonged Pu'u 'O'o eruption of Kilauea Volcano, Hawaii. *J. Pet.* 41, 967–990.
- Gerlach, T.M., McGee, K.A., Elias, T., Sutton, A.J., Doukas, M.P., 2002. Carbon dioxide emission rate of Kilauea

- Volcano: implications for primary magma and the summit reservoir. *J. Geophys. Res.* 107.
- Giordano, D., Dingwell, D.B., 2003. Viscosity of hydrous Etna basalt: implications for Plinian-style basaltic eruptions. *Bull. Volcanol.* 65, 8–14.
- Goldstein, P., Chouet, B., 1994. Array measurements and modeling of sources of shallow volcanic tremor at Kilauea Volcano, Hawaii. *J. Geophys. Res.* 99, 2637–2652.
- Gonnermann, H.M., Manga, M., 2007. The fluid mechanics inside a volcano. *Ann. Rev. Fluid Mech.* 39, 321–356.
- Gonnermann, H.M., Houghton, B.F., Sable, J.E. The Plinian eruption of basalt magma. *J. Geophys. Res.*, in press.
- Gresta, S., Pipepe, M., Marchetti, E., D'Amico, S., Coltelli, M., Harris, A.J.L., Privitera, E., 2004. Seismacoustic measurements during the July–August 2001 eruption of Mt. Etna volcano, Italy. *J. Volcanol. Geotherm. Res.* 137, 219–230.
- Guet, S., Ooms, G., 2006. Fluid mechanical aspects of the gas-lift technique. *Annu. Rev. Fluid Mech.* 38, 225–249.
- Guet, S., Decarre, S., Henriot, V., Line, A., 2006. Void fraction in vertical gas–liquid slug flow: influence of liquid slug content. *Chem. Eng. Sci.* 61, 7336–7350.
- Gurioli, L., Harris, A., Houghton, B.F., Polacci, M., Ripepe, M. Textural and geophysical characterization of explosive basaltic activity at Villarrica volcano. *J. Geophys. Res.*, in press.
- Harris, A., Ripepe, M., 2007. Temperature and dynamics of degassing at Stromboli. *J. Geophys. Res.* 112, B03205.
- Hauri, E., 2002. SIMS analysis of volatiles in silicate glasses. 2: Isotopes and abundances in Hawaiian melt inclusions. *Chem. Geol.* 183, 115–141.
- Heiken, G., Wohletz, K., 1985. *Volcanic Ash*: Berkley. University of California Press, 246pp.
- Heliker, C.C., Mangan, M.T., Mattox, T.N., Kauahikaua, J.P., Helz, R.T., 1998. The character of long-term eruptions: inferences from episodes 50–53 of the Pu'u 'O'o-Kupaianaha eruption of Kilauea Volcano. *Bull. Volcanol.* 59, 381–393.
- Heliker, C.C., Kauahikaua, J., Sherrod, D.R., Lisowski, M., Cervelli, P.F., 2003. The Rise and fall of Pu'u 'O'o Cone, 1983–2002. US Geological Survey Professional Paper 1676, pp. 29–51.
- Hewitt, G.F., 1990. Non-equilibrium two-phase flow. In: *Proceedings of the 9th International Heat Transfer Conference* vol. 1, 383–394.
- Hibiki, T., Ishii, M., 2003a. One-dimensional drift-flux model and constitutive equations for relative motion between phases in various two-phase flow regimes. *Int. J. Heat Mass Transfer* 46, 4935–4948.
- Hibiki, T., Ishii, M., 2003b. One-dimensional drift-flux model for two-phase flow in a large diameter pipe. *Int. J. Heat Mass Transfer* 46, 1773–1790.
- Hoskuldsson, A., Oskarsson, N., Pedersen, R., Gronvold, K., Vogfjoro, K., Olafsdottir, R., 2007. The millennium eruption of Hekla in February 2000. *Bull. Volcanol.* 70, 169–182.
- Houghton, B.F., Wilson, C.J.N., Smith, I.E.M., 2000. Shallow-seated controls on styles of explosive basaltic volcanism: a case study from New Zealand. *J. Volcanol. Geotherm. Res.* 91, 97–120.
- Houghton, B.F., Wilson, C.J.N., Del Carlo, P., Coltelli, M., Sable, J.E., Carey, R.J., 2004. The influence of conduit processes on changes in style of basaltic Plinian eruptions: Tarawera 1886 and Etna 122 BC. *J. Volcanol. Geotherm. Res.* 137, 1–14.
- Hu, B., Golan, M., 2004. Dynamic simulator predicts gas lift well instability. *J. Pet. Technol.* 56.
- Hui, H.J., Zhang, Y.X., 2007. Toward a general viscosity equation for natural anhydrous and hydrous silicate melts. *Geochim. Cosmochim. Acta* 71, 403–416.
- Huppert, H.E., Woods, A.W., 2002. The role of volatiles in magma chamber dynamics. *Nature* 420, 493–495.
- Ida, Y., 2007. Driving force of lateral permeable gas flow in magma and the criterion of explosive and effusive eruptions. *J. Volcanol. Geotherm. Res.* 162, 172–184.
- James, M.R., Lane, S.J., Chouet, B., Gilbert, J.S., 2004. Pressure changes associated with the ascent and bursting of gas slugs in liquid-filled vertical and inclined conduits. *J. Volcanol. Geotherm. Res.* 129, 61–82.
- James, M.R., Lane, S.J., Chouet, B.A., 2006. Gas slug ascent through changes in conduit diameter: laboratory insights into a volcano-seismic source process in low-viscosity magmas. *J. Geophys. Res.* 111.
- Jaupart, C., Vergnolle, S., 1988. Laboratory models of Hawaiian and Strombolian eruptions. *Nature* 331, 58–60.
- Jaupart, C., Vergnolle, S., 1989. The generation and collapse of a foam layer at the roof of a basaltic magma chamber. *J. Fluid Mech.* 203, 347–380.
- Johnson, M.C., Anderson, A.T., Rutherford, M.J., 1994. Pre-eruptive volatile contents of magmas, volatiles in magmas. *Rev. Min.* 30, 281–330.
- Kamenetsky, V.S., Pompilio, M., Metrich, N., Sobolev, A.V., Kuzmin, D.V., Thomas, R., 2007. Arrival of extremely volatile-rich high-Mg magmas changes explosivity of Mount Etna. *Geology* 35, 255–258.
- Koyaguchi, T., 2005. An analytical study for 1-dimensional steady flow in volcanic conduits. *J. Volcanol. Geotherm. Res.* 143, 29–52.
- Landi, P., Metrich, N., Bertagnini, A., Rosi, M., 2004. Dynamics of magma mixing and degassing recorded in plagioclase at Stromboli (Aeolian Archipelago, Italy). *Cont. Min. Pet.* 147, 213–227.
- Lautze, N.C., Houghton, B.F., 2005. Physical mingling of magma and complex eruption dynamics in the shallow conduit at Stromboli volcano, Italy. *Geology* 33, 425–428.
- Lautze, N.C., Houghton, B.F., 2006. Linking variable explosion style and magma textures during 2002 at Stromboli volcano, Italy. *Bull. Volcanol.* 69, 445–460.
- Lautze, N.C., Houghton, B.F., 2007. Single explosions at Stromboli in 2002: use of clast microtextures to map physical diversity across a fragmentation zone. *J. Volcanol. Geotherm. Res.* doi:10.1016/j.jvolgeores.2007.10.011.
- Lavallee, Y., Hess, K.U., Cordonnier, B., Dingwell, D.B., 2007. Non-Newtonian rheological law for highly crystalline dome lavas. *Geology* 35, 843–846.
- La Volpe, L., Manetti, P., Trigila, R., Villari, L., 1999. *Volcanology and chemistry of the Earth's interior: Italian research activity (1995–1998) report to IAVCEI.* *Boll. Geof. Teor. App.* 40, 163–298.

- Lejeune, A.M., Richet, P., 1995. Rheology of crystal-bearing silicate melts – an experimental study at high viscosities. *J. Geophys. Res.* 100, 4215–4229.
- Lejeune, A.M., Bottinga, Y., Trull, T.W., Richet, P., 1999. Rheology of bubble-bearing magmas. *Earth Planet. Sci. Lett.* 166, 71–84.
- Llewellyn, E.W., Manga, A., 2005. Bubble suspension rheology and implications for conduit flow. *J. Volcanol. Geotherm. Res.* 143, 205–217.
- Llewellyn, E.W., Mader, H.M., Wilson, S.D.R., 2002. The rheology of a bubbly liquid. *Proc. R. Soc. Lond.* 458, 987–1016.
- Lockwood, J.P., Dvorak, J.J., English, T.T., Koyanagi, R.Y., Okamura, A.T., Summers, M.L., Tanigawa, W.R., 1987. Mauna Loa 1974–1984: a decade of intrusive and extrusive activity. In: Decker, R.W., Wright, T.L., Stauffer, P.H. (Eds.), *Volcanism in Hawai'i*, US Geological Survey Professional Paper 1350, pp. 537–570.
- Macdonald, G.A., Abbott, E.T., Peterson, F.L., 1984. *Volcanoes in the Sea. The Geology of Hawaii*. University of Hawaii Press, Honolulu, p. 517.
- Mangan, M.T., Cashman, K.V., 1996. The structure of basaltic scoria and reticulite and inferences for vesiculation, foam formation, and fragmentation in lava fountains. *J. Volcanol. Geotherm. Res.* 73, 1–18.
- Manga, M., Loewenberg, M., 2001. Viscosity of magmas containing highly deformable bubbles. *J. Volcanol. Geotherm. Res.* 105, 19–24.
- Mangan, M.T., Cashman, K.V., Newman, S., 1993. Vesiculation of basaltic magma during eruption. *Geology* 21, 157–160.
- Marchetti, E., Ripepe, M., 2005. Stability of the seismic source during effusive and explosive activity at Stromboli Volcano. *Geophys. Res. Lett.* 32.
- McBirney, A.R., Murase, T., 1970. Factors governing the formation of pyroclastic rocks. *Bull. Volcanol.* 34, 372–384.
- McMillan, P.F., 1994. Water solubility and speciation models, volatiles in magmas. *Rev. Min.* 30, 131–156.
- McNeil, D.A., Stuart, A.D., 2003. The effects of a highly viscous liquid phase on vertically upward two-phase flow in a pipe. *Int. J. Heat Mass Transfer* 29, 1523–1549.
- McNeil, D.A., Stuart, A.D., 2004. Vertically upward two-phase flow with a highly viscous liquid-phase in a nozzle and orifice plate. *Int. J. Heat Mass Transfer* 25, 58–73.
- Melnik, O., Sparks, R.S.J., 2002. Dynamics of magma ascent and lava extrusion at Soufriere Hills Volcano, Montserrat. In: Druitt, T.H., Kokelaar, B.P. (Eds.), *The Eruption of Soufriere Hills Volcano, Montserrat, from 1995 to 1999*. Geological Society, London, pp. 153–171.
- Melnik, O., Barmin, A.A., Sparks, R.S.J., 2005. Dynamics of magma flow inside volcanic conduits with bubble overpressure buildup and gas loss through permeable magma. *J. Volcanol. Geotherm. Res.* 143, 53–68.
- Menand, T., Phillips, J.C., 2007. Gas segregation in dykes and sills. *J. Volcanol. Geotherm. Res.* 159, 393–408.
- Meriaux, C., Jaupart, C., 1995. Simple fluid dynamic models of volcanic rift zones. *Earth Planet. Sci. Lett.* 136, 223–240.
- Metrich, N., Rutherford, M.J., 1998. Low pressure crystallization paths of H₂O-saturated Basaltic-Hawaiitic melts from Mt Etna: implications for open-system degassing of basaltic volcanoes. *Geochim. Cosmochim. Acta* 62, 1195–1205.
- Metrich, N., Bertagnini, A., Landi, P., Rosi, M., 2001. Crystallization driven by decompression and water loss at Stromboli Volcano (Aeolian Islands, Italy). *J. Pet.* 42, 1471–1490.
- Metrich, N., Allard, P., Spilliaert, N., Andronico, D., Burton, M., 2004. 2001 flank eruption of the alkali- and volatile-rich primitive basalt responsible for Mount Etna's evolution in the last three decades. *Earth Planet. Sci. Lett.* 228, 1–17.
- Metrich, N., Bertagnini, A., Landi, P., Rosi, M., Belhadj, O., 2005. Triggering mechanism at the origin of paroxysms at Stromboli (Aeolian Archipelago, Italy): the 5 April 2003 eruption. *Geophys. Res. Lett.* 32, 4.
- Mitchell, K.L., 2005. Coupled conduit flow and shape in explosive volcanic eruptions. *J. Volcanol. Geotherm. Res.* 143, 187–203.
- Namiki, A., Manga, M., 2005. Response of a bubble bearing viscoelastic fluid to rapid decompression: implications for explosive volcanic eruptions. *Earth Planet. Sci. Lett.* 236, 269–284.
- Namiki, A., Manga, M., 2008. Transition between fragmentation and permeable outgassing of low viscosity magmas. *J. Volcanol. Geotherm. Res.* 169, 48–60.
- Newman, S., Lowenstern, J.B., 2002. VOLATILECALC: a silicate melt–H₂O–CO₂ solution model written in Visual Basic for excel. *Comp. Geosci.* 28, 597–604.
- Ornebère-Iyari, N.K., Azzopardi, B.J., Ladam, Y., 2007. Two-phase flow patterns in large diameter vertical pipes at high pressures. *AIChE J.* 53, 2493–2504.
- Pal, R., 2002. Complex shear modulus of concentrated suspensions of solid spherical particles. *J. Colloid Interface Sci.* 245, 171–177.
- Pal, R., 2003. Rheological behavior of bubble-bearing magmas. *Earth Planet. Sci. Lett.* 207, 165–179.
- Pal, R., 2004. Rheological constitutive equation for bubbly suspensions. *Ind. Eng. Chem. Res.* 43, 5372–5379.
- Papale, P., 1999. Strain-induced magma fragmentation in explosive eruptions. *Nature* 397, 425–428.
- Papale, P., 2005. Determination of total H₂O and CO₂ budgets in evolving magmas from melt inclusion data. *J. Geophys. Res.* 110.
- Papale, P., Moretti, R., Barbato, D., 2006. The compositional dependence of the saturation surface of H₂O + CO₂ fluids in silicate melts. *Chem. Geol.* 229, 78–95.
- Parfitt, E.A., 1998. A study of clast size distribution, ash deposition and fragmentation in a Hawaiian-style volcanic eruption. *J. Volcanol. Geotherm. Res.* 84, 197–208.
- Parfitt, E.A., 2004. A discussion of the mechanisms of explosive basaltic eruptions. *J. Volcanol. Geotherm. Res.* 134, 77–107.
- Parfitt, E.A., Wilson, L., 1995. Explosive volcanic eruptions – IX. The transition between Hawaiian-style lava fountaining and Strombolian explosive activity. *Geophys. J. Int.* 121, 226–232.
- Parfitt, E.A., Wilson, L., 1999. A Plinian treatment of fallout from Hawaiian lava fountains. *J. Volcanol. Geotherm. Res.* 88, 67–75.
- Parfitt, E.A., Wilson, L., Head, J.W., 1993. Basaltic magma reservoirs – factors controlling their rupture characteristics and evolution. *J. Volcanol. Geotherm. Res.* 55, 1–14.

- Parfitt, E.A., Wilson, L., Neal, C.A., 1995. Factors influencing the height of Hawaiian lava fountains: implications for the use of fountain height as an indicator of magma gas content. *Bull. Volcanol.* 57, 440–450.
- Park, J.W., Lahey, R.T.J., Drew, D.A., 1993. The measurement of void waves in bubbly two-phase flows. In: *Proceedings of the 6th International Meeting on Nuclear Reactor Thermal-Hydraulics*, pp. 655–662.
- Patrick, M.R., 1996. Strombolian eruption dynamics from thermal (FLIR) video imagery. Unpublished Ph.D. dissertation. Department of Geology & Geophysics, University of Hawaii.
- Patrick, M.R., Harris, A.J.L., Ripepe, M., Dehn, J., Rothery, D., Calvari, S., 2007. Strombolian explosive styles and source conditions: insights from thermal (FLIR) video. *Bull. Volcanol.* 69, 769–784.
- Perez, W.A., Freundt, A., 2006. The youngest highly explosive basaltic eruptions from Masaya Caldera (Nicaragua): stratigraphy and hazard assessment. *Geol. Soc. Am. Bull.* 412, 189–207.
- Phillips, J.C., Woods, A.W., 2001. Bubble plumes generated during recharge of basaltic magma reservoirs. *Earth Planet. Sci. Lett.* 186, 297–309.
- Pinel, V., Jaupart, C., 2004a. Likelihood of basaltic eruptions as a function of volatile content and volcanic edifice size. *J. Volcanol. Geotherm. Res.* 137, 201–217.
- Pinel, V., Jaupart, C., 2004b. Magma storage and horizontal dyke injection beneath a volcanic edifice. *Earth Planet. Sci. Lett.* 221, 245–262.
- Polacci, M., Corsaro, R.A., Andronico, D., 2006. Coupled textural and compositional characterization of basaltic scoria: insights into the transition from Strombolian to fire fountain activity at Mount Etna, Italy. *Geology* 34, 201–204.
- Polacci, M., Baker, D.R., Bai, L., Mancini, L., 2008. Large vesicles record pathways of degassing at basaltic volcanoes. *Bull. Volcanol.* doi:10.1007/s00445-007-0184-8.
- Proussevitch, A.A., Sahagian, D.L., Anderson, A.T., 1993. Dynamics of diffusive bubble growth in magmas: isothermal case. *J. Geophys. Res.* 98, 22283–22307.
- Pyle, D.M., 1989. The thickness, volume and grain-size of tephra fall deposits. *Bull. Volcanol.* 51, 1–15.
- Pyle, D.M., Pyle, D.L., 1995. Bubble migration and the initiation of volcanic-eruptions. *J. Volcanol. Geotherm. Res.* 67, 227–232.
- Radovcich, N.A., Moissis, R., 1962. The transition from two-phase bubble flow to slug flow. MIT Report 7-7373-22.
- Richter, D.H., Eaton, J.P., Murata, K.J., Ault, W.U., Krivoy, H.L., 1970. Chronological narrative of the 1959–60 eruption of Kilauea volcano, Hawaii. US Geological Survey Professional Paper 537-E, 73.
- Ripepe, M., Gordeev, E., 1999. Gas bubble dynamics model for shallow volcanic tremor at Stromboli. *J. Geophys. Res.* 104, 10639–10654.
- Ripepe, M., Marchetti, E., 2002. Array tracking of infrasonic sources at Stromboli volcano. *Geophys. Res. Lett.* 29.
- Ripepe, M., Rossi, M., Saccorotti, G., 1993. Image-processing of explosive activity at Stromboli. *J. Volcanol. Geotherm. Res.* 54, 335–351.
- Ripepe, M., Ciliberto, S., Della Schiava, M., 2001. Time constraints for modeling source dynamics of volcanic explosions at Stromboli. *J. Geophys. Res.* 106, 8713–8727.
- Ripepe, M., Marchetti, E., Olivieri, G., Harris, A.J.L., Dehn, J., Burton, M., Caltabiano, T., Salerno, G., 2005. Effusive to explosive transition during the 2003 eruption of Stromboli volcano. *Geol. Soc. Am. Bull.* 33, 341–344.
- Roggensack, K., Hervig, R.L., McKnight, S.B., Williams, S.N., 1997. Explosive basaltic volcanism from Cerro Negro volcano: influence of volatiles on eruptive style. *Science* 277, 1639–1642.
- Rosi, M., Bertagnini, A., Landi, P., 2000. Onset of the persistent activity at Stromboli Volcano (Italy). *Bull. Volcanol.* 62, 294–300.
- Rosi, M., Bertagnini, A., Harris, A.J.L., Pioli, L., Pistolesi, M., Ripepe, M., 2006. A case history of paroxysmal explosions at Stromboli: timing and dynamics of the April 5, 2003 event. *Earth Planet. Sci. Lett.* 243, 594–606.
- Saar, M.O., Manga, M., Cashman, K.V., Fremouw, S., 2001. Numerical models of the onset of yield strength in crystal-melt suspensions. *Earth Planet. Sci. Lett.* 187, 367–379.
- Sable, J.E., Houghton, B.F., Del Carlo, P., Coltelli, M., 2006a. Changing conditions of magma ascent and fragmentation during the Etna 122 BC basaltic Plinian eruption: evidence from clast microtextures. *J. Volcanol. Geotherm. Res.* 158, 333–354.
- Sable, J.E., Houghton, B.F., Wilson, C.J.N., Carey, R.J., 2006b. Complex proximal sedimentation from Plinian plumes: the example of Tarawera 1886. *Bull. Volcanol.* 69, 89–103.
- Sable, J.E., Houghton, B.F., Wilson, C.J.N., Carey, R.J. Eruption mechanisms during the climax of the Tarawera 1886 basaltic Plinian. *Geol. Soc. Lond. Spec. Pub.*, in press.
- Saiz-Jabardo, J.M., Bouré, J.A., 1989. Experiments on void fraction waves. *Int. J. Multiphase Flow* 15, 483–493.
- Schmincke, H.U., 2004. *Volcanism*. Springer, Berlin, Federal Republic of Germany, p. 324.
- Scollo, S., Del Carlo, P., Coltelli, M., 2007. Tephra fallout of 2001 Etna flank eruption: analysis of the deposit and plume dispersion. *J. Volcanol. Geotherm. Res.* 160, 147–164.
- Self, S., Sparks, R.S.J., Booth, B., Walker, G.P.L., 1974. The 1973 Heimaey Strombolian scoria deposit, Iceland. *Geol. Mag.* 111, 539–548.
- Shamberger, P.J., Garcia, M.O., 2006. Geochemical modeling of magma mixing and magma reservoir volumes during early episodes of Kilauea Volcano's Pu'u 'O'o eruption. *Bull. Volcanol.* 69, 345–352.
- Shimozuru, D., 1994. Physical parameters governing the formation of Pele's hair and tears. *Bull. Volcanol.* 56, 217–219.
- Simakin, A.G., Salova, T.P., 2004. Plagioclase crystallization from a Hawaiian melt in experiments and in a volcanic conduit. *Petrology* 12, 82–92.
- Sisson, T.W., Grove, T.L., 1993. Temperatures and H₂O contents of low-MgO high-alumina basalts. *Cont. Min. Pet.* 113, 167–184.
- Slezin, Y.B., 2003. The mechanism of volcanic eruptions (a steady state approach). *J. Volcanol. Geotherm. Res.* 122, 7–50.

- Sparks, R.S.J., 1978. The dynamics of bubble formation and growth in magmas: a review and analysis. *J. Volcanol. Geotherm. Res.* 3, 1–37.
- Sparks, R.S.J., Pinkerton, H., 1978. Effect of degassing on rheology of basaltic lava. *Nature* 276, 385–386.
- Sparks, R.S.J., Barclay, J., Jaupart, C., Mader, H.M., Phillips, J.C., 1994. Physical Aspects of Magmatic Degassing. Experimental and Theoretical Constraints on Vesiculation, Volatiles in Magmas: *Reviews in Mineralogy*, vol. 30. Mineral. Soc. America, Washington, DC, pp. 413–445.
- Spieler, O., Kennedy, B., Kueppers, U., Dingwell, D.B., Scheu, B., Taddeucci, J., 2004. The fragmentation threshold of pyroclastic rocks. *Earth Planet. Sci. Lett.* 226, 139–148.
- Spilliaert, N., Allard, P., Metrich, N., Sobolev, A.V., 2006a. Melt inclusion record of the conditions of ascent, degassing, and extrusion of volatile-rich alkali basalt during the powerful 2002 flank eruption of Mount Etna (Italy). *J. Geophys. Res.* 111.
- Spilliaert, N., Metrich, N., Allard, P., 2006b. S-G-F degassing pattern of water-rich alkali basalt: modelling and relationship with eruption styles on Mount Etna volcano. *Earth Planet. Sci. Lett.* 248, 772–786.
- Stasiuk, M.V., Barclay, J., Carroll, M.R., Jaupart, C., Ratté, J.C., Sparks, R.S.J., Tait, S.R., 1996. Degassing during magma ascent in the Mule Creek vent (USA). *Bull. Volcanol.* 58 (2/3), 117–130.
- Stevenson, R.J., Dingwell, D.B., Webb, S.L., Sharp, T.G., 1996. Viscosity of microlite-bearing rhyolitic obsidians: an experimental study. *Bull. Volcanol.* 58, 298–309.
- Swanson, D.A., Duffield, W.A., Jackson, D.B., Peterson, R.W., 1979. Chronological narrative of the 1969–71 Mauna Ulu eruption of Kilauea volcano, Hawaii. U.S.G.S. Professional Paper 1056, 55pp.
- Taddeucci, J., Pompilio, M., Scarlato, P., 2002. Monitoring the explosive activity of the July–August 2001 eruption of Mt. Etna (Italy) by ash characterization. *Geophys. Res. Lett.* 29, X1–X4.
- Taddeucci, J., Pompilio, M., Scarlato, P., 2004a. Conduit processes during the July–August 2001 explosive activity of Mt. Etna (Italy): inferences from glass chemistry and crystal size distribution of ash particles. *J. Volcanol. Geotherm. Res.* 137, 33–54.
- Taddeucci, J., Spieler, O., Kennedy, B.M., Pompilio, M., Dingwell, D.B., Scarlato, P., 2004b. Experimental and analytical modeling of basaltic ash explosions at Mount Etna, Italy, 2001. *J. Geophys. Res.* 109, B08203.
- Tait, S., Jaupart, C., Vergnolle, S., 1989. Pressure, gas content and eruption periodicity of a shallow, crystallizing magma chamber. *Earth Planet. Sci. Lett.* 92, 107–123.
- Taitel, Y., Bornea, D., Dukler, A.E., 1980. Modeling flow pattern transitions for steady upward gas–liquid flow in vertical tubes. *AIChE J.* 26, 345–354.
- Thorarinnsson, S., Steinthorsson, S., Einarsson, T.H., Kristmannsdottir, H., Oskarsson, N., 1973. The eruption of Heimaey, Iceland. *Nature* 241, 372–375.
- Thordarson, T., Self, S., 1993. The Laki (Skaftár Fires) and Grimsvötn eruption of 1783–1785 and associated phenomena. *Bull. Volcanol.* 54, 233–263.
- Tutu, N.K., 1982. Pressure-fluctuations and flow pattern-recognition in vertical 2 phase gas–liquid flows. *Int. J. Multiphase Flow* 8, 443–447.
- Tutu, N.K., 1984. Pressure-drop fluctuations and bubble-slug transition in a vertical 2-phase air water-flow. *Int. J. Multiphase Flow* 10, 211–216.
- Vergnolle, S., Brandeis, G., 1994. Origin of the sound generated by Strombolian explosions. *Geophys. Res. Lett.* 21, 1959–1962.
- Vergnolle, S., Caplan-Auerbach, J., 2006. Basaltic thermals and subplinian plumes: constraints from acoustic measurements at Shishaldin volcano, Alaska. *Bull. Volcanol.* 68, 611–630.
- Vergnolle, S., Jaupart, C., 1986. Separated two-phase flow and basaltic eruptions. *J. Geophys. Res.* 91, 12842–12860.
- Vergnolle, S., Jaupart, C., 1990. Dynamics of degassing at Kilauea Volcano, Hawaii. *J. Geophys. Res.* 95, 2793–2809.
- Vergnolle, S., Mangan, M., 2000. Hawaiian and Strombolian eruptions. In: Sigurdsson, H. (Ed.), *Encyclopedia of Volcanoes*. Academic Press, San Diego, CA, pp. 447–461.
- Vergnolle, S., Brandeis, G., Mareschal, J.C., 1996. Strombolian explosions. 2. Eruption dynamics determined from acoustic measurements. *J. Geophys. Res.* 101, 20449–20466.
- Vergnolle, S., Boichu, M., Caplan-Auerbach, J., 2004. Acoustic measurements of the 1999 basaltic eruption of Shishaldin volcano, Alaska-1. Origin of Strombolian activity. *J. Volcanol. Geotherm. Res.* 137, 109–134.
- Verhoogen, J., 1951. Mechanics of ash formation. *Am. J. Sci.* 249, 729–739.
- Villermaux, E., 2007. Fragmentation. *Ann. Rev. Fluid Mech.* 39, 419–446.
- Wade, J.A., Plank, T., Melson, W.G., Soto, G.J., Hauri, E.H., 2006. The volatile content of magmas from Arenal volcano, Costa Rica. *J. Volcanol. Geotherm. Res.* 157, 94–120.
- Walker, G.P.L., 1973. Explosive volcanic eruptions – a new classification scheme. *Geol. Rund.* 62, 431–446.
- Walker, G.P.L., Croasdale, R., 1972. Characteristics of some basaltic pyroclastics. *Bull. Volcanol.* 35, 303–317.
- Walker, G.P.L., Self, S., Wilson, L., 1984. Tarawera 1886, New Zealand – a basaltic plinian fissure eruption. *J. Volcanol. Geotherm. Res.* 21, 61–78.
- Wallace, P.J., 2005. Volatiles in subduction zone magmas: concentrations and fluxes based on melt inclusion and volcanic gas data. *J. Volc. Geotherm. Res.* 140, 217–240.
- Wallace, P.J., Anderson, A.T., 1998. Effects of eruption and lava drainback on the H₂O contents of basaltic magmas at Kilauea Volcano. *Bull. Volcanol.* 59, 327–344.
- Wallis, G.B., 1969. *One-Dimensional Two-Phase Flow*. McGraw-Hill.
- Webb, S.L., Dingwell, D.B., 1990. The onset of non-Newtonian rheology of silicate melts – a fiber elongation study. *Phys. Chem. Miner.* 17, 125–132.
- Wehrmann, H., Bonadonna, C., Freundt, A., Houghton, B.F., Kutterolf, S., 2006. Fontana Tephra: a basaltic Plinian eruption in Nicaragua. *Geological Society of America* 412, 209–223.
- Williams, S.N., 1983. Plinian airfall deposits of basaltic composition. *Geology* 11, 211–214.
- Wilson, L., 1980. Relationships between pressure, volatile content and ejecta velocity in 3 types of volcanic explosion. *J. Volcanol. Geotherm. Res.* 8, 297–313.

- Wilson, L., 1999. Explosive volcanic eruptions. X. The influence of pyroclast size distributions and released magma gas contents on the eruption velocities of pyroclasts and gas in Hawaiian and Plinian eruptions. *Geophys. J. Int.* 136, 609–619.
- Wilson, L., Head, J.W., 1981. Ascent and eruption of basaltic magma on the Earth and Moon. *J. Geophys. Res.* 86, 2971–3001.
- Wilson, L., Head, J.W., 1983. A comparison of volcanic-eruption processes on Earth, Moon, Mars, Io and Venus. *Nature* 302, 663–669.
- Wilson, L., Head, J.W., 2001. Lava fountains from the 1999 Tvashtar Catena fissure eruption on Io: implications for dike emplacement mechanisms, eruption rates, and crystal structure. *J. Geophys. Res.* 106, 32997–33004.
- Wilson, L., Walker, G.P.L., 1987. Explosive volcanic eruptions – VI. Ejecta dispersal in plinian eruptions: the control of eruption conditions and atmospheric properties. *Geophys. J. R. Astron. Soc.* 89, 657–679.
- Wolfe, E.W., Garcia, M.O., Jackson, D.B., Koyanagi, R.Y., Neal, C.A., Okamura, A., 1987. The Puu Oo eruption of Kilauea Volcano, episodes 1–20, January 3, 1983, to June 8, 1984. In: Decker, R.W., Wright, T.L., Stauffer, P.H. (Eds.), *Volcanism in Hawaii: US Geological Survey Professional Paper 1350*, pp. 471–508.
- Woods, A.W., Cardoso, S.S.S., 1997. Triggering basaltic volcanic eruptions by bubble–melt separation. *Nature* 385, 518–520.
- Woods, A.W., Bokhove, O., de Boer, A., Hill, B.E., 2006. Compressible magma flow in a two-dimensional elastic-walled dike. *Earth Planet. Sci. Lett.* 246, 241–250.
- Zhang, Y.X., 1999. A criterion for the fragmentation of bubbly magma based on brittle failure theory. *Nature* 402, 648–650.
- Zimanowski, B., Buttner, R., Lorenz, V., Hafele, H.G., 1997. Fragmentation of basaltic melt in the course of explosive volcanism. *J. Geophys. Res.* 102, 803–814.